



Delft University of Technology

Photocatalyst-Incorporated Cross-Linked Porous Polymer Networks

Esen, Cansu; Kumru, Baris

DOI

[10.1021/acs.iecr.2c01658](https://doi.org/10.1021/acs.iecr.2c01658)

Publication date

2022

Document Version

Final published version

Published in

Industrial and Engineering Chemistry Research

Citation (APA)

Esen, C., & Kumru, B. (2022). Photocatalyst-Incorporated Cross-Linked Porous Polymer Networks. *Industrial and Engineering Chemistry Research*, 61(30), 10616-10630. <https://doi.org/10.1021/acs.iecr.2c01658>

Important note

To cite this publication, please use the final published version (if applicable). Please check the document version above.

Copyright

Other than for strictly personal use, it is not permitted to download, forward or distribute the text or part of it, without the consent of the author(s) and/or copyright holder(s), unless the work is under an open content license such as Creative Commons.

Takedown policy

Please contact us and provide details if you believe this document breaches copyrights. We will remove access to the work immediately and investigate your claim.

Photocatalyst-Incorporated Cross-Linked Porous Polymer Networks

Cansu Esen and Baris Kumru*



Cite This: *Ind. Eng. Chem. Res.* 2022, 61, 10616–10630



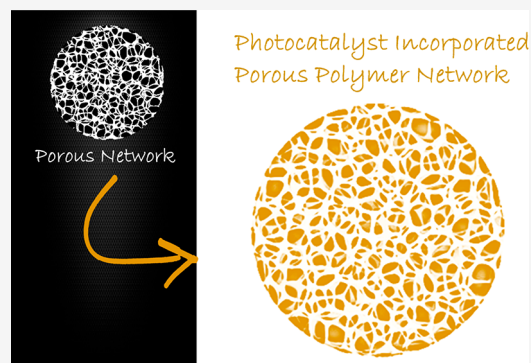
Read Online

ACCESS |

Metrics & More

Article Recommendations

ABSTRACT: The utilization of sunlight to conduct chemistry has been on a stark rise in the era of sustainability. A similar trend is observed in polymer science, mainly to initiate polymerization and modify polymer materials, but mostly relying on the utilization of soluble initiator/activator molecules. Semiconductors, on the other hand, grant a platform for “photoredox” induced chemical pathways, so that reductive and oxidative reactions (as well as radical formation) can be tailored according to band positions. Despite their utilization as dispersed or dissolved phases, immobilization of semiconductors on macroscale solid surfaces is attractive to entail scale-up options. In this Review, semiconductors incorporated in cross-linked porous polymer networks will be summarized both from synthesis and application perspectives.



INTRODUCTION

Versatility in polymer synthesis distilled a field of cross-linked polymer networks.¹ Despite their discovery and large-scale utilization long ago, cross-linked polymers keep receiving attention.^{2,3} These materials possess stability against solvents and environmental effects, as well as exhibit dimensional stability.^{4,5} The majority of cross-linked polymers can be considered as thermosets. The vulcanization of rubber can be a benchmark example for such systems,⁶ or epoxy thermosets that serve as a matrix for aviation composites. From a synthetic point of view, cross-linking can be achieved via methods such as covalent and noncovalent. Covalent cross-linking aims to form a linkage between independent polymer chains. Some synthetic examples on covalent cross-linking are (i) carbon–carbon bond formation,^{7–9} (ii) carbon–heteroatom bond formation,^{10–12} and (iii) various other approaches, such as S–S bond¹³ and tertiary amine–halogen quaternization.¹⁴ It is important to note that some covalent cross-linking can possess dynamic reversible nature, as in the case of S–S bonds. Noncovalent cross-linking donates a generally “reversible” property, in a way that the supramolecular forces–interactions building the network can be influenced. The most dominating choices to generate supramolecular cross-linking are hydrogen bonding,¹⁵ electrostatic interactions,¹⁶ π interactions,¹⁷ and host–guest mechanisms.^{18,19}

Macroscale cross-linked porous polymer networks can be classified by the nature of polymer chains in a way that a library of materials based on aqueous-air nature (i.e., hydrogels,^{20,21} aerogels²²), organic nature (i.e., resins,²³ organogels²⁴), and silicon-based nature (i.e., (polydimethylsiloxane)s²⁵) exist. The porosity of aforementioned networks is identified via “swelling” and “solvent uptake” parameters. When utilized for catalytic

purposes, accessible porosity and an interlinked channel formation in these networks possess a significant value. Potential application of cross-linked porous polymers relies on the nature of the polymer, thermomechanical properties and its affinity for solvents. While hydrogels are attractive for tissue engineering²⁶ and wound dressing,²⁷ organic resins are employed as column fillers²⁸ and catalyst supports,²⁹ whereas aerogels and PDMS sponge materials are preferred based on their superior structural and thermal stability.^{30,31}

Natural photosynthesis has been an inspiration to scientists to develop light-driven reactions. Billions of years of evolution optimized working system with active centers, enzymes, and membranes to reach unprecedented performances based on converting CO₂ into hydrocarbons and oxygen.³² The natural process starts with complicated visible-light induced water oxidation to O₂ and four electrons–four protons that are guided by natural membranes for optimized charge separation,³³ which then are consumed in a Calvin cycle with CO₂ to form oxygen and hydrocarbons.³⁴ Cited references exceptionally summarize natural photocatalytic reactions in detail. Photocatalytic reactions such as water splitting aims to perform in a similar manner; therefore, an interest in photocatalytically active materials started. Semiconductors possess prime importance in daily life as they are mainly employed in electronic devices.³⁵ On an electron conductivity

Received: May 10, 2022

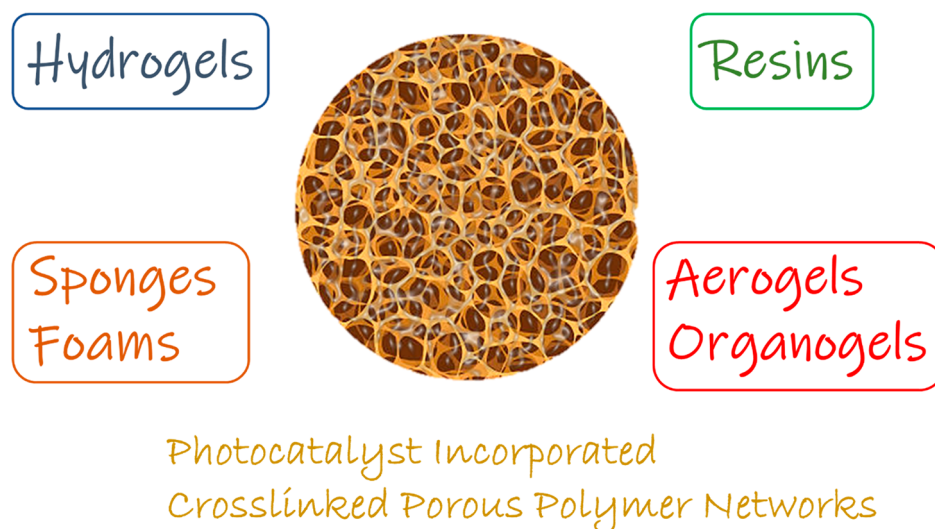
Revised: July 7, 2022

Accepted: July 11, 2022

Published: July 20, 2022



Scheme 1. A Sketch of Crosslinked Porous Polymer Network and Subjects That Will Be Covered in This Review



scale, they lie between conductors and insulators, hence their fundamental properties arise from there.³⁶ Since the discovery of photoactivity of TiO₂ for water photolysis via photoredox reactions in 1972, the impact of semiconductors in photocatalysis flourished.³⁷ Semiconductors are defined with their corresponding bandgap (and light absorption), when a light in an absorption range hits a semiconductor, an electron (e⁻) is excited to the conduction band (CB), leaving a positive hole (h⁺) in the valence band (VB).³⁸ Thus, two oppositely charged species (e⁻ and h⁺) are formed, and the term “photoredox” corresponds to possible reductive (via e⁻) and oxidative (h⁺) chemical reactions.³⁹ Formation of intermediate active species, such as radicals and singlet oxygen, rely on tailoring reaction parameters (solvent, sacrificial agents etc.).⁴⁰ In this way, photoredox chemistry differs from other mechanisms (radical initiators, etc.) as more-complex chemical routes can produce a library of possible reactions.⁴¹ One of the key parameters for photoactivity is the charge separation so that e⁻ and h⁺ must be separated to retain activity. There are several strategies to enhance charge separation which can be found in the literature.^{42,43} Recombination is an unwanted situation where e⁻ and h⁺ combines, which results in no photoactivity.⁴⁴ It is important to note that processes described here occur within nanoseconds. Semiconductors can be classified as elements (Si, Ge), inorganic materials (i.e., TiO₂, CdS, perovskites, InP, ZnO, ZnS, Cu₂O, SnO₂, BaTiO₃), organic materials (i.e., polymeric carbon nitrides, soluble dyes, xanthenes), and precious-metal complexes (Ir complexes, etc.). When one designs a semiconductor, it is very crucial to elucidate its properties. The synthesis and characterization of semiconductors require a joint input from chemistry and physics. While element- and metal-based systems are restricted by means of tunability (one can tune grain size, crystallinity, surface etc.), polymeric carbon nitride stands out, since it represents a family of materials.⁴⁵ Hence, by rational design approach, it is possible to tune many parameters such as conductivity, charge separation, crystallinity, porosity, absorption, dispersibility, and sheet size.^{46–48} Some of the most popularized photoredox-based applications of semiconductors include water splitting,^{49–51} organic synthesis,^{52,53} photovoltaics,^{54,55} environmental remediation,⁵⁶ CO₂ photoreduc-

tion,⁵⁷ polymer synthesis,^{58–60} and photoelectrochemical transformations.^{61,62}

The potential impact of semiconductors can be addressed via their utilized form, such as homogeneous or heterogeneous. On a simple glance, heterogeneous catalysis provides ease of removal and recyclability, compared to homogeneous catalysis.⁶³ Furthermore, employing semiconductors in their dispersed (colloidal) state offers novel avenues of application.⁶⁴ Because of the fact that the semiconductors described previously are mainly consisting of inorganic crystal and conjugated polymer structures, their utilization lies on the colloidal state. However, on a large scale, using nanosized or micrometer-sized powder photocatalysts bear significant disadvantages, especially in purification, which would be costly in terms of energy and time. To amplify their features, semiconductors have been incorporated into polymer materials to form macroscale photoactive hybrids. Recently, there have been valuable articles on semiconductor-embedded polymer composite films^{65–69} and composite nanoparticles;^{70–73} however these will be excluded in the current Review. In addition, we would like to direct readers into photocatalyst-coated glass,^{74–76} clay,^{77,78} and silica gel⁷⁹ beads that are designed for scaled-up photocatalytic reactions.

In this Review, we will provide a perspective on the incorporation of semiconductors on macroscale porous polymer networks, and their potential applications will be covered (Scheme 1). It is important to note that carbonaceous materials, metal–organic frameworks (MOFs) and covalent organic frameworks (COFs) can be considered as nanoscale porous polymers. However, this minireview will focus on synthetic polymer chemistry; therefore, it is aimed toward macroscale porous polymer materials. In addition, photoactivity can be introduced via organic modifications on native polymer chains.⁸⁰ However, this will be mainly beyond the scope of the current review.

■ HYDROGELS

Hydrogels possess 3D macroporous structure with high affinity to water. Polymer chains are hydrophilic; thus, it is possible to afford functional soft materials. Many traditional covalent hydrogels can be prepared via free-radical polymerization, using a big library of hydrophilic vinyl-based monomers and

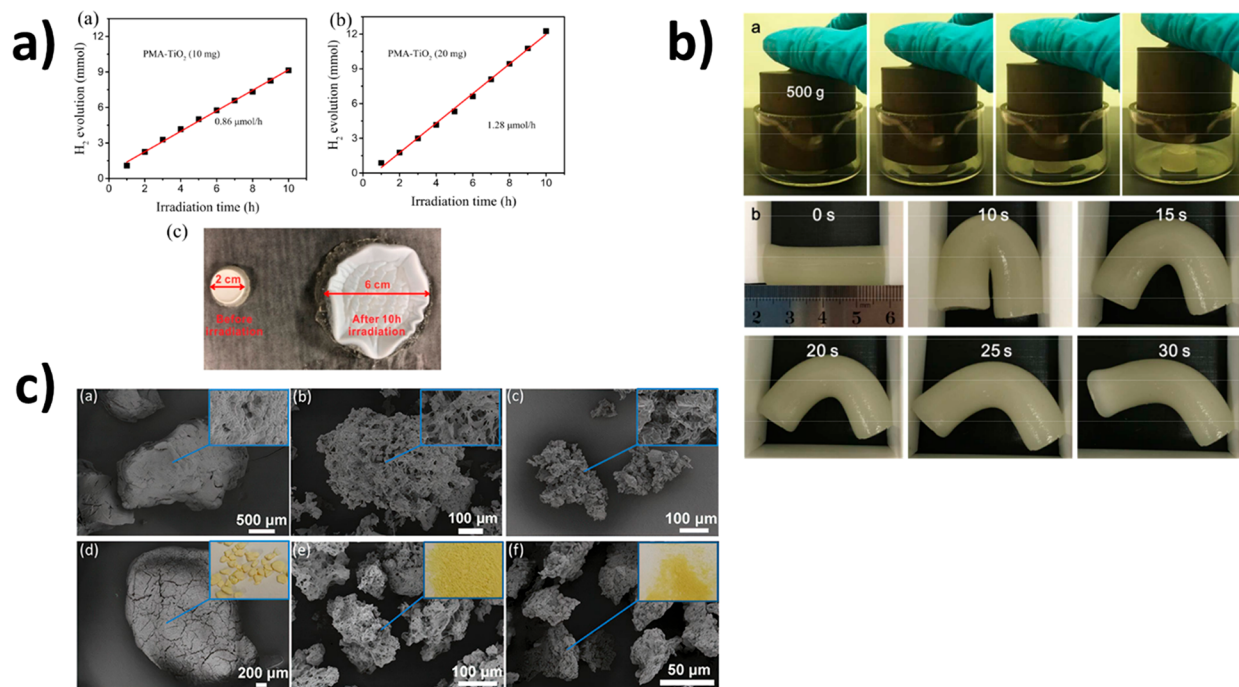


Figure 1. (a) Photocatalytic hydrogen production from water using TiO₂ containing hydrogels with varied TiO₂ amounts (TiO₂ amount doubled on right curve) and digital image of photoactive hydrogel before and after photocatalytic reaction [obtained from ref 84, published open access under CC-BY, copyright 2021, MDPI]. (b) Digital images of photoactive hydrogel cylinder against 500 g load (top) and tubular photoactive hydrogel against compression and its recovery (bottom) [adapted with permission from ref 85, copyright 2017, American Chemical Society, Washington, DC]. (c) SEM images of photoactive porous hydrogel beads (with varied g-CN content and cross-linker amount) obtained via inverse suspension polymerization [obtained from ref 87, published open access under CC-BY, copyright 2020, American Chemical Society, Washington, DC].

cross-linkers; hence, simplicity offers an attractive subject to be studied. Despite their massive popularity in tissue engineering and absorption on an industrial scale, macroscale hydrogels can be ideal hosts to accommodate photoactive materials to access novel applications. Because of their hydrophilic nature, hydrogel-based photoactive composites can exhibit unprecedented activities in aqueous applications.⁸¹

A representative example for supramolecular hydrogel (SMH)-based photocatalyst elucidates fabrication of Ag₂O/alginate (ALG) SMH films via a solution casting process. In this method, Na⁺ in alginate was replaced with Ag⁺, which led to the formation of an interwoven network, followed by in situ transformation of Ag⁺ into Ag₂O after irradiation in water. In this way, Ag₂O could be successfully maintained in as-prepared composite films, thanks to both ALG, which accommodates photoformed holes, and O₂, which captures photoformed electrons generated via Ag₂O under light irradiation. Regarding this, photoactivity of Ag₂O/ALG SMH composite films were investigated by Methylene Blue (MB) and Malachite Green (MG) dye photodegradation experiments. In conclusion, all results showed very high activities (above 93% for both dyes under either UV or visible-light irradiation).⁸²

TiO₂/agarose hybrid gel photocatalyst was prepared via simple gelation of agarose gel with uniformly dispersed TiO₂ NPs in hot water. This thermal construction method is followed by a cooling step and fractionation of the hybrid gel in capsule form as a final step. The overall process has shown very effective encapsulation of TiO₂ NPs, as well as recovery via simple separation from the matrix. Excellent recovery of TiO₂ NPs in monolithic hybrid gel resulted in enhanced photodegradation of MB dye and its degradation rate was

investigated by varied concentration, size, and uniformity of the hybrid gel.⁸³ An alternative to immobilization of TiO₂ NPs in hydrogel network was also achieved via an embedding technique. Two hydrogel supports based on poly(methyl acrylate) (PMA) and succinamic acid (SAA) combined with TiO₂ NPs during the gelation step, and the resulting composite hydrogel-TiO₂ samples exhibited preferable photodegradation for four organic dyes (MO, MB, RhB, and bright green) under UV light irradiation, in addition to promising H₂ generation that can be improved by optimizing sample transparency in order to harvest more incident light (Figure 1a).⁸⁴ Design strategy by using nanoparticles highly rely on colloidal dispersions and colloidal stabilities, as sedimentation of particles cause lowered photoactivities, despite having high solid contents.

Metal-free semiconductor graphitic carbon nitride has been a popular choice for hydrogel matrices recently. Since g-CN is a conjugated sheetlike semiconductor, mechanical reinforcements in hybrid hydrogels, compared to pristine ones, were the focus of some studies; however, we will stress photoactive hydrogel composites here. In one study, three-dimensional (3-D) g-CN-based self-standing hydrogels were fabricated via photopolymerization in plastic syringes, where g-CN can be employed as a colloidal photoinitiator. The obtained hybrid hydrogel photocatalysts were immersed in a mixture of various cationic and ionic dyes to prove the selective adsorption properties of as-synthesized hybrid hydrogels over counterion attraction (the best result was obtained using MB, and the rest of employed dyes were Congo Red, Crystal Violet, Methyl Orange, Rhodamine B). Furthermore, a set of dye-absorbed hydrogels exhibited enhanced dye photodegradation under

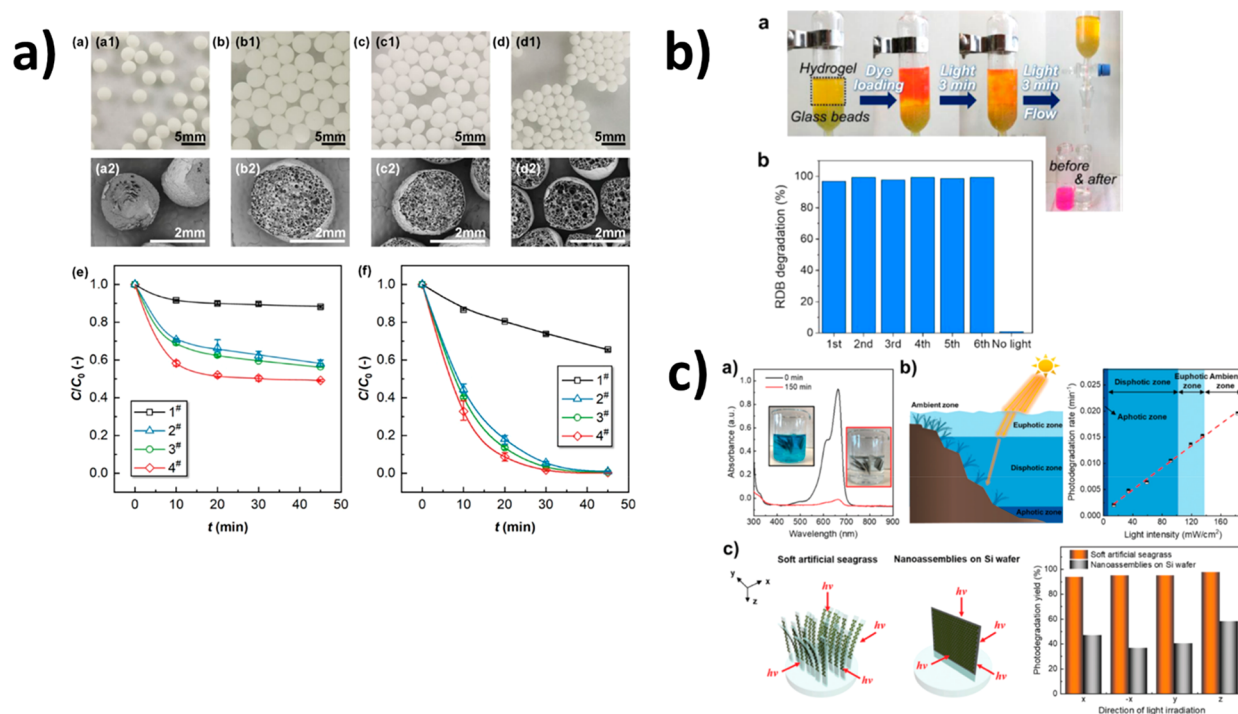


Figure 2. (a) Digital images and SEM images of g-CN-based photoactive CO₂-induced porous hydrogels synthesized via tunable parameters and their influence on photocatalytic RhB degradation [adapted with permission from ref 89, copyright 2021, American Chemical Society, Washington, DC]. (b) Digital image of photoactive hydrogel beads in column for RhB photodegradation as well as recyclability data [obtained from ref 93, published under CC-BY, copyright 2019, American Chemical Society, Washington, DC]. (c) Photoactive hydrogel composite in dye removal and the influence of light intensity and direction on photocatalytic reaction inspired by natural seagrass [adapted with permission from ref 100, copyright 2021, Royal Society of Chemistry, London].

visible-light illumination. Furthermore, authors demonstrated the potential of photocatalytic hydrogen generation from water under visible light by designing a tubelike hydrogel model in order to tackle thickness issues (Figure 1b).⁸⁵ Photoactivity of hydrogel can be harnessed to form double network-like systems. The stability of g-CN in monomer-cross-linker aqueous dispersion systems diminish upon the addition of charged monomers, thus restricting admission to functional systems. To overcome this, g-CN-based prepolymer was synthesized (g-CN dispersion in water:ethylene glycol:monomer, followed by irradiation under continuous stirring), which possesses high viscosity yet improved colloidal stability against charged molecules. For the formation of a secondary network, the g-CN-based prepolymer was mixed with an anionic monomer (3-sulfopropyl methacrylate potassium salt) in the presence of water and cross-linker, and visible-light irradiation forms a double network-like polymer that has cartilage-like toughness and lubricity.⁸⁶ In these studies, once again, stable colloidal dispersions are key enablers for the successful immobilization of semiconductors; in addition, the photoactivity of the semiconductor was harnessed to form a hydrogel network in the initial stage.

To switch from bulk systems to heterophase polymerization, g-CN incorporated macrohydrogel beads were synthesized via inverse suspension photopolymerization technique, in which water-dispersible g-CN was employed in the aqueous phase with ethylene glycol and water-soluble acrylamide monomer in a continuous oil phase prepared using cyclohexane and various amounts of cross-linker (acrylamide based). In this heterophase polymerization, g-CN was utilized as photoinitiator in fabricating hybrid macrogels in various sizes (from 30 μm to 4

mm) that can be tuned via parameters such as cross-linker ratio and agitation speed. Photoactivity of hybrid hydrogel beads were elucidated via RhB photodegradation as well as hydrogen generation under visible light, with a good recyclability and reliability, unlike powder g-CN (Figure 1c).⁸⁷ However, obtaining a perfect bead shape was not possible, because structural deformations occurred during polymerization.

Synthetic conditions might be altered by embedding g-CN nanosheets during hydrogelation. g-CN embedded highly porous hydrogels (DMA/MBA combination) were synthesized using redox-couple (ascorbic acid/hydrogen peroxide) radical initiation under dark conditions in a Petri dish (completed in 3 h). Following that, subsequent in situ surface photomodification transforms g-CN-embedded hydrogel into “hydrophobic hydrogel” relying on accessible g-CN allocation over the hydrogel network. According to results, obtained high porosity eased light reachability so that light can reflect through the network and ease the interaction with g-CN nanosheets, which are responsible for initiating radical formation for in situ photomodification. It is demonstrated that resulting “hydrophobic hydrogel” can be employed for agricultural applications to simulate a nutrition release system in a controlled way. In addition to “hydrophobic hydrogel” fabrication, parental g-CN embedded hydrogel is swollen by various acrylate monomers via immersion, and, under visible-light irradiation, secondary polymer networks were formed, resulting in “pore substructuring”.⁸⁸

CO₂ can help forming porosity in macroscale structures, as shown in fabrication of g-CN-immobilized alginate porous gel beads. Aqueous dispersion of g-CN nanosheets (CNNSs) were mixed with sodium alginate (NaAlg) solution containing

sodium dodecyl sulfate (SDS) and sodium bicarbonate (NaHCO_3) under agitation until a foamy solution is obtained. Thereafter, as-prepared solution was treated with calcium chloride/acetic acid ($\text{CaCl}_2/\text{CH}_3\text{COOH}$) solution by dripping using an automated syringe. This process solidifies droplets on the interface and builds interconnected porosity inside (CO_2 released from the reaction between CH_3COOH and NaHCO_3) (Figure 2a). Interconnected macroporosity with accessible semiconductor sides resulted in RhB photodegradation activities.⁸⁹

The heterojunction of g-CN with silver halide in a water-permeable cross-linked CMC (carboxy methyl cellulose) matrix showed remarkable photocatalytic performance with regard to RhB dye photodegradation (60 min, 74% efficiency). Photoactive CMC-based hydrogels prepared via the addition of AlCl_3 or FeCl_3 ($\text{Ag}/\text{AgCl}@/\text{Al-CMC}$ and $\text{AgCl}@/\text{Fe-CMC}$, respectively) to entrap AgCl formation during interconnected cross-linking. The overall benefit of silver species in photocatalytic applications, especially zerovalent silver that significantly reduce the electron–hole recombination rate, worked quite effectively after successful combination with Fe^{3+} , which act as electron trapping sites in a CMC network. As a result, both $\text{Ag}/\text{AgCl}@/\text{Al-CMC}$ and $\text{AgCl}@/\text{Fe-CMC}$ hybrid samples exhibited remarkable photocatalytic performance under visible-light irradiation (98% and 87% of RhB dye removal efficiency in 60 min, respectively).⁹⁰

Sulfide-based semiconductors are often employed in hydrogel systems as well. In the first example, a hydrogel matrix was produced by $\text{Co-}\gamma$ radiation-induced copolymerization, and CuS loading was performed via an in-situ precipitation method which eventuated as a hybrid hydrogel photocatalyst (p(HEA/NMMA)-CuS) successfully. Subsequently, the resulting novel photocatalyst was used in the adsorption and degradation of sulfamethoxazole (SMX) in aqueous solution. Briefly, sulfonamide antibiotics (SAs) are commonly known with their difficulty of degradation and these aqueous micropollutants pose danger for society by causing resistivity against drugs along with rapid bacteria growth. SMX is a compound that is primarily found in the water resources; therefore, it has been chosen to be employed as a model compound in photocatalytic investigations. Regarding the photocatalytic degradation process, the hybrid hydrogel adsorbed SMX molecules, which enhanced the physical contact with CuS under visible-light irradiation. Total photodegradation of SMX molecules down to water and CO_2 was based on photo-generated electrons and holes formed after exciting CuS nanoparticles (OH^- and the H_2O molecules generated hydroxyl radicals via oxidation and, thereafter, holes and $\bullet\text{OH}$ radicals attack SMX molecules). According to the results, p(HEA/NMMA)-CuS photocatalyst hydrogel degraded SMX in an aqueous solution under visible light within 24 h at a removal ratio of 95.91%, as well as reaching 43.56% of mineralized SMX ratio. Theoretical calculations of frontier electron densities (FEDs) regarding possible degradation routes of SMX intermediates were also presented and discussed precisely.⁹¹

In the second example, almost the same preparation route was followed to synthesize hydrogel via $\text{Co-}\gamma$ radiation-induced copolymerization and then an in-situ precipitation method for loading CdS nanoparticles, resulting in a photoactive composite named P(HEA-co-HAM)-CdS , and is conducted for the removal of bisphenol A (BPA). Results of BPA adsorption from aqueous solution and in situ photocatalytic

degradation under visible-light irradiation were successful since the adsorption capacity of P(HEA-co-HAM)-CdS hydrogel was much higher than that of similar adsorbents (11.26 mg/g), and BPA degradation and mineralization rates reaching 92% and 47% within 3 h, respectively. Degradation pathways were discussed both theoretically and experimentally.⁹²

It is crucial to retain hydrophilicity in order to maximize semiconductor contact in aqueous media. Considering this, a translucent conjugated polymer hydrogel photocatalyst (P-BT-GX), possessing ionic as well as cationic sides (therefore also named as conjugated polyelectrolyte) prepared by a successful complexation of a photoactive polycation and various amounts of poly(acrylic acid) (polyanion). This voluminous water-compatible photocatalyst (deionized water absorption up to 470 times its weight) exhibited enhanced RhB dye degradation and the formation of enzyme cofactor nicotinamide adenine dinucleotide (NAD^+) via photo-oxidation in water, under adequate visible-light irradiation (Figure 2b). NADH photo-oxidation was described in detail by starting with cationic radical ($\text{NADH}^{\bullet+}$) formation via photogenerated holes from P-BT-GX , which further transforms to NAD^+ via superoxide radical (formed from molecular oxygen quenched with photogenerated electrons). Accumulation of perhydroxyl radicals as side products led to the generation of peroxide molecules that can form hydroxyl radicals, and those hydroxyl radicals captured proton from $\text{NADH}^{\bullet+}$ that of involved oxidation of NAD^+ . In addition, a facile solvent exchange method exhibited profitable regeneration of as-prepared hydrogel photocatalyst.⁹³

In another example with polyelectrolyte (PE) hydrogel as photocatalyst matrix, chromophore amphiphile (CA) photocatalyst was integrated via self-assembly based on both electrostatic interactions and physical entrapment. Presynthesized PE covalent hydrogel (via free-radical polymerization) as host platform, combined with monomeric perylene monoimide (PMI) CA via solvent exchange method from organic to water led to their successful self-assembly. Obtained hybrid hydrogels demonstrated noticeable photocatalytic hydrogen production, good reusability with enhanced mechanical strength, and partial retention of CA assemblies (ribbon-like nanostructures obtained via coarse-grained molecular dynamics simulations) even after a thorough washing process (retention was expected from a system where the assemblies are not covalently attached to the hydrogel network).⁹⁴

Since we have briefly referenced the importance of light accessibility in photobased applications, a recent study showed the remarkable impact of highly transparent matrix obtained via DMAA-based hydrogel, which, when further cross-linked with benzothiadiazole and employed in the photo-oxidation of glyphosate (N -(phosphonomethyl)glycine), RhB dye, organic sulfurs, and photoreduction of Cr^{VI} . The overall results were all successful, clearly highlighting the importance of light penetration into hydrogel matrix to maximize light–semiconductor contact.⁹⁵

Hydrophobic association hydrogels (HyA) are the type of hydrogel that are built on hydrophobic interactions. This physical cross-linking intrinsically endowed high mechanical properties as well as effective self-healing properties to the final material. In this particular study, TiO_2 nanoparticles were associated as both photoinitiators and physical cross-linking points in the fabrication of $\text{TiO}_2/\text{HyA-n}$ hydrogels through in situ radical polymerization. By this strategy, remarkable mechanical behavior (tensile strength of 306 kPa, compressive

strength of 2.17 MPa) as well as advantageous antifatigue property and excellent photocatalytic activity (MB photodegradation rate = 96.63%) were obtained from a tough hybrid photoactive hydrogel.⁹⁶

The removal of organic contaminants from wastewaters is a complex task when powder photocatalysts are used, mainly due to separation problems. Hydrophilic hydrogels endowed with photoactivity can offer improved performances and stability. Two significant examples combined a microfluidics technique to form photocatalyst-encapsulated polymer particles as an alternative to slurry or fixed batch reactors. Furthermore, reliable high-throughput-production technologies were demonstrated. In the first example, a mixture of acrylate derived monomers (HEMA, AA, EGDMA), cross-linker (DMPA) and dispersion of TiO₂ nanoparticles (5–15 nm anatase) prepared in aqueous media and after radical initiator addition, hydrogel–TiO₂ composite was obtained via photopolymerization in a PDMS mold designed for the scale of a microreactor (via a two-step soft lithography process). Resulting hydrogel scaffolds were tunable despite ionic strength (AA volume fraction) and pore sizes, which are capable of transmitting incident visible light as well as ultraviolet (UV) light, showed remarkable permeability of MB and its further photodegradation under UV light irradiation. In addition, a photocatalytic hydrogel reactor was examined in norfloxacin (type of pharmaceutical that can be detected in wastewaters and has a similar photodegradation behavior with MB) removal, in a channel with a continuous flow of water. Related results exhibited that, despite the lower photodegradation rate of norfloxacin compared to MB, composite hydrogel shows promising data as photoactive microreactor composites possess better transport phenomena.⁹⁷ In the second example, TiO₂ and ZnO nanoparticles encapsulated in poly(methacrylic acid)-based hydrogel, termed as photocatalyst-in-capsule (PIC), via complex water-in-oil-in-water double emulsions produced by glass capillary microfluidic device. The fabrication starts with the photopolymerization of methacrylic anhydride (MAN) and ethylene glycol dimethacrylate (EGDMA), which results in a poly(anhydride) structure in shell, whereas an aqueous dispersion of photocatalyst is located at the core. Photopolymerization and further hydrolyses yield poly(methacrylic acid) hydrogel photoactive microcapsules successfully. According to the results, photocatalytic nanoparticles in thin-shell hydrogel microcapsules photodegraded MB dye quite effectively, based on the adsorption–oxidation mechanism, which is comparable to powder photocatalysis. A flow reactor filled with hydrogel microcapsules also showed effective water purification performance.⁹⁸

Reduced graphene hydrogel (rGH) was demonstrated as a suitable platform for quantum dots (QDs) decoration. Briefly, in this study, QDs self-decorated BiVO₄ NPs structure was coupled to rGH hydrogel by in situ growth method. The highly porous rGH network that was obtained showed well distribution of BiVO₄ NPs but QDs on both sides of rGH sheets. Fabricated composite succeeded tetracycline hydrochloride (TC.HCl) photodegradation via visible-light irradiation, thanks to the highly effective photoinduced charge carrier separation achieved by rapid migration of electrons to the rGH surface. Composite also exhibited significant stability and reusability up to four cycles with no structural change. As a conclusion, this QD self-decoration over graphene hydrogel network approach has proven once again the advantage of hydrogel structure as a support platform for enhanced

photocatalytic efficiency.⁹⁹ Despite having benefits of having graphene as an electron acceptor agent in hydrogel systems, having much graphene would significantly lower light absorption to photoactive moieties.

Being inspired by the nature, especially on the subject of photobased applications referred in this Review, can pave the way of novel material design (Figure 2c). A seagrass-like structure was fabricated first by constructing monodisperse Au–Pd–CdS multifunctional nanohexagons (mNHs) (via a seed-mediated method, using gold nanohexagons (Au NHs) as seeds), followed by polyvinylpyrrolidone (PVP) modification and casting on aluminum for nanoassembly. Drop-casting 1% agarose aqueous solution and heating leads to gelation after the removal of aluminum foil which gives free-standing nanoassembly-based photoactive composite. Regarding the concept, plasmonic nanoparticles (gold nanohexagons (NHs)) possessed corner-specific deposition of Pd nanoparticles meanwhile semiconductor (CdS nanoparticles) integration occurs over the surfaces. Hydrogel hybrid showed high photocatalytic performance on MB photodegradation by omnidirectional light-harvesting feature under low-intensity sunlight irradiation, since it was aimed to mimic natural seagrasses. In the study, it was stressed that fabricated seagrass-like material had superior recycling and flexibility and did not require photocatalyst regeneration, which means it is fully capable to run continuous photocatalytic operations.¹⁰⁰

Another example on solvothermal method shows the combination of carboxymethyl cellulose and poly(β -cyclodextrin) hydrogel support with photoactive metal organic framework (MIL-101(Fe)) (CMC/MIL-101(Fe)/ β -CDP). β -CDP as a host material features a hydrophilic surface with a hydrophobic cavity that accommodates MIL-101(Fe) in the cavities, and the final composite with CMC significantly enhanced the selective oxidation of tetracycline under visible-light illumination due to lower electron/hole recombination supported by β -CDP as a promoter matrix (Table 1).¹⁰¹

Table 1. Summary of Fabrication Methods for Photoactive Hydrogel Systems

reference(s)	fabrication method
82	supramolecular attachment of semiconductor precursor into alginate
83, 84, 88–90, 97, 98, 100, 101	gelation of semiconductor dispersion (embedding/encapsulation)
85–87, 96	gelation by photoinitiation using semiconductors as photoinitiators
91, 92	in-situ precipitation of semiconductors within gel network
93	charge complexation
94	solvent exchange on host network to introduce photoactive material
95	organic photoactive moiety is in monomer unit
99	in-situ growth of semiconductor within reduced graphene hydrogel

■ ORGANOGELS–AEROGELS

Thermal insulation and mechanical features primarily define aerogel materials. Generally, aerogels are fabricated via a solvent removal process from hydrogel/organogel networks. Organogel formation is a supramolecular process that relies on convenient gelator agents in organic solvents. These networks, as host materials for semiconductors, can offer many features,

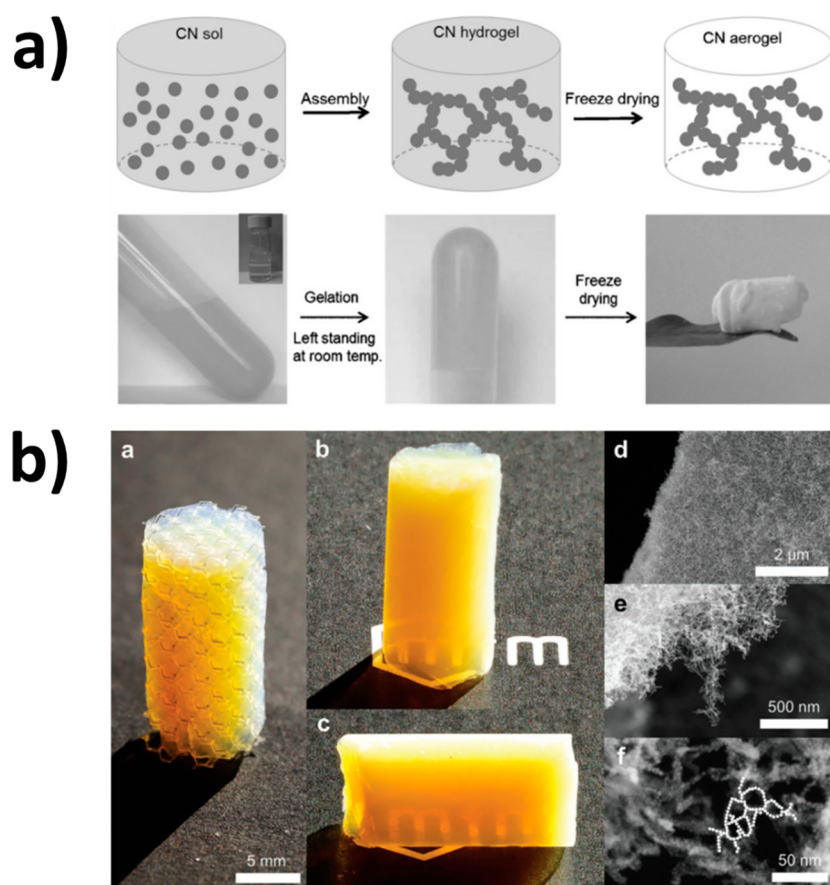


Figure 3. (a) Schematic description and digital images of g-CN-based aerogel synthesis [adapted with permission from ref 103, copyright 2017, John Wiley and Sons]. (b) Digital images and SEM images of 3D-printed photocatalytic aerogels [obtained from ref 105, published under CC-BY-NC, copyright 2021, John Wiley and Sons].

such as interconnected large surface areas, ease of recyclability, and mechanical stability.¹⁰² A self-supported macroscopic carbon nitride (CN) aerogel was fabricated via an aqueous sol–gel technique that requires neither an external cross-linking agent nor strong acid treatment, unlike traditional methods. Principles of colloid chemistry were entailed in this approach, such that the self-assembly of low-density CN nanoparticles (LD CN NPs) in aqueous media first formed hydrogel, which was subsequently transformed to a pure CN aerogel by freeze-drying (Figure 3a). The photoactive three-dimensional (3D) monolithic aerogel network exhibited enhanced hydrogen evolution and H₂O₂ production under visible light, compared to bulk CN, mainly due to the functional groups that are introduced, high internal surface area, increased carrier conduction ability, and improved physical property.¹⁰³ However, structural stability is desired. In another study, a polysulfone–alginate matrix (PSF 10:6 Alg) was converted to visible-light-responsive composite beads (PATAg, with an outer diameter (od) of ~3 mm), via the successful immobilization of TiO₂/Ag₃PO₄ (10:1, 12 wt %) semiconductor nanocomposite via assembly. The resulting PATAg beads, possessing interconnected macrovoids (more dominant) led by the presence of PSF at the backbone and micropores via Alg contribution, have shown unique adhesion of catalyst, in addition to high adsorption capacity and buoyancy-suspension interconversion. As a proof of concept, photodegradation of wastewater pollutant (MB) and pharmaceutical contaminants (diclofenac and triclosan) in suspended

form, as well as water disinfection (bacterial inactivation) and biofilm retardation (decomposition of acyl-homoserine lactones) under visible-light irradiation, noted the photocatalytic activity of hybrid PATAg beads.¹⁰⁴ Alternatively, upgrading mechanical properties of nanoparticle-based aerogels via introducing 3D printed polymeric scaffolds for gas-phase reactions is a further example that reveals the versatility of aerogels. A 3D-printed resin scaffold was treated with a TiO₂–Pd dispersion, followed by solvent exchange and supercritical drying, to obtain a photoactive aerogel.

3D printing allows precise control on channel structure to optimize gas flow–photocatalyst contact to boost the photocatalytic activity with a minimized waste (Figure 3b). Consolidating hierarchical architecture of aerogel with tunable polymeric scaffolds allowed TiO₂–Pd-based photocatalytic aerogels to be highly efficient in reformation of methanol for H₂ production through gas flow reactor under UV light illumination.¹⁰⁵ However, transparency is hindered which restricts light penetration and prevents the full potential of 3D-printed photoactive aerogel. In macro or/and larger scale, supramolecular gels combined with semiconductors have shown immense impact on photobased applications. Their reversible nature, based on assembly–disassembly equilibrium via noncovalent interactions (hydrogen bonding, p–p stacking, donor–acceptor interactions, metal coordination, hydrophobic forces, van der Waals interactions) allows further reactions in confined spaces, which plays a key role in tuning photocatalytic activity of desired materials.¹⁰⁶ Low-molecular-weight com-

pounds (LMWCs) formed through self-aggregation of small gelator molecules resulting in entangled self-assembled fibrillar networks (SAFINs) that originated from photon upconversion based on triplet–triplet annihilation (TTA-UC) techniques once they are successfully incorporated with semiconductors. A good example is prepared from transparent bile-organogelator (derived from dimeric urea) integrated with luminescent CdSe quantum dots (QDs) showed a well-defined QD array in the resulting hybrid–SAFIN network formed via supramolecular assembly (Table 2).¹⁰⁷ Moreover, QD-doped SAFIN exhibited

Table 2. Summary of Fabrication Methods for Photoactive Organogel–Aerogel Systems

reference	fabrication method
103	self-assembly of semiconducting nanoparticles
104	assembly of semiconductor composite on bead surface
105	3D printing
107	supramolecular assembly of organogel network with semiconducting QDs

thermoreversible luminescent features based on enhanced rigidification of QD over the network; however, authors did not include photocatalysis in this project.

■ SPONGES/FOAMS

When “sponge” or “sponge-like” materials are mentioned in materials science, polydimethylsiloxane (PDMS)-based ones are, by far, the most studied. Different than foams (fabricated by blowing agents leading to the generation of gaseous molecules creating bubbles), silicone-based sponges are mainly synthesized via two techniques: the “open-cell method”, which leads to interconnected porosity, or the “closed-cell method”, which creates isolated cell formation over the structure. Either way, the 3D stochastic cellular scaffolds obtained exhibiting hierarchical porosity draws attention in photocatalysis, especially given the fact that enhanced binding sites for an efficient mass transfer throughout the sponge channels. Various methods in the fabrication of PDMS photocatalysts have been reported so far. In a recently published review, the three most common techniques were briefly summarized: (i) the incorporation of photocatalyst into liquid PDMS monomer before curing, (ii) the deposition of photocatalyst particles onto cured PDMS thermoset support, and (iii) the coating of the photocatalyst with PDMS. Besides providing the opportunity to be fabricated in various ways, PDMS sponge as host material inherently endows numerous advantages in photocatalytic applications, e.g., (I) super hydrophobic properties, which are quite substantial in attracting organic pollutants that can donate an increase in photocatalytic efficiency; (II) transparent feature that facilitates accessibility of light; (III) robustness and chemical resistivity, which, in return, boosts photocatalyst recyclability; and (IV) facile preparation methods at low cost.¹⁰⁸

A prominent example of PDMS-supported photocatalyst, TiO₂–SiO₂@PDMS hybrid prepared via a sol–gel process (silica and titania gel first functionalized with hexamethyldisilazane then dispersed in PDMS/CHCl₃, followed by curing), has shown efficient photocatalytic activity for MB photodegradation performed in both aqueous dye solution and MB-dyed films. Besides, hybrid photocatalytic powder exhibited superhydrophobicity (water contact angle (WCA) < 5°) and good thermal stability (470 °C).¹⁰⁹ In other work, a PDMS

sponge (prepared via a conventional sugar template method) was dipped into hydrocarbon/TiO₂ nanoparticle solution (in IPA), sonicated, and dried for successful coating; hence, the resulting nanosponge/porous polydimethylsiloxane (NS/p-PDMS) composite exhibited UV-induced wetting transition property. Superhydrophobic nature arising from hydrocarbon functionalities on NS/p-PDMS as well as PDMS structure itself, led to selective oil absorption in aqueous media which exhibited a remarkable air-bubble-driven desorption mechanism under UV light irradiation. This photoresponsive behavior over oil absorption/desorption proved the versatility of the fabricated NS/p-PDMS hybrid photocatalyst.¹¹⁰ Another article features a composite TiO₂–PDMS sponge fabricated via hexamethyldisilazane (HMDS)-functionalized TiO₂ NPs injection on an as-prepared PDMS sponge (sugar templating method) at various ratios, that not only demonstrated high adsorption against Rhodamine B dye (TiO₂–PDMS sponge is embedded in dye solution) but also exhibited high efficiency in photo degradation of adsorbed dye molecules via solar light irradiation. Embodying hydrophobic –CH₃ groups over TiO₂ NPs clearly enhanced the interaction between PDMS matrix as well as increased the attraction of organic dye molecules for a higher photodegradation rate.¹¹¹

For an improved photocatalytic activity, PDMS–TiO₂ sponge is treated with Au NPs solution (HAuCl₄·3H₂O in anhydrous EtOH) by injection, followed by a drying process (60 °C–6 h) to obtain PDMS–TiO₂–Au composite sponge. The host PDMS–TiO₂ network was obtained via slightly modified sugar cube templating to allow maximized access of Au NPs on TiO₂ rich interface. This strategy led to create highly effective floating porous plasmonic photocatalyst thanks to localized surface plasmon resonance (LSPR) effect arising from Au NPs under visible-light irradiation (red-shifted in comparison to PDMS–Au sponge). In principle, excited surface plasmons of Au NPs generate hot electrons that either can be directly involved into catalytic cycle or form electron–hole couples after contacting TiO₂ NPs. This way, even though TiO₂ NPs have an insufficient conduction band to generate electron–hole pairs under visible light, Au NPs integration on PDMS–TiO₂ showed significant photocatalytic activity, even without the need of photosensitization (concluded via decomposition of MB dye under 513 nm light illumination).¹¹² In another example referring enhanced charge carrier mobility over fast recombination of electron–hole pairs, a surfactant wrapping sol–gel method for the fabrication of multiple-walled carbon nanotubes/titanium dioxide (MWCNTs/TiO₂) nanocomposites on PDMS via needle-based microfluidic device was reported. The resulting PDMS–MWCNTs/TiO₂ microdroplets (oil-in-water single emulsion template method) transformed to microparticles after thermal curing and showed a strong synergetic effect for azo-type dye sorption and degradation under UV light illumination. In this way, the advantage of immobilized TiO₂ NPs over CNTs substrate that acts as an electron acceptor paved the way to higher photocatalytic activity, compared to the solo performance of TiO₂ NPs. In addition, microfluidic system inherently provided more controllability over droplet formations and lower consumption of reactants.¹¹³

Benefits of TiO₂ NPs in photobased applications certainly set forward designing photoactive hybrid and composite materials; however, when TiO₂ abundance and toxicity is considered, various semiconductors by merit takes the role, such as ZnO. As an example, PDMS/ZnO composite sponge

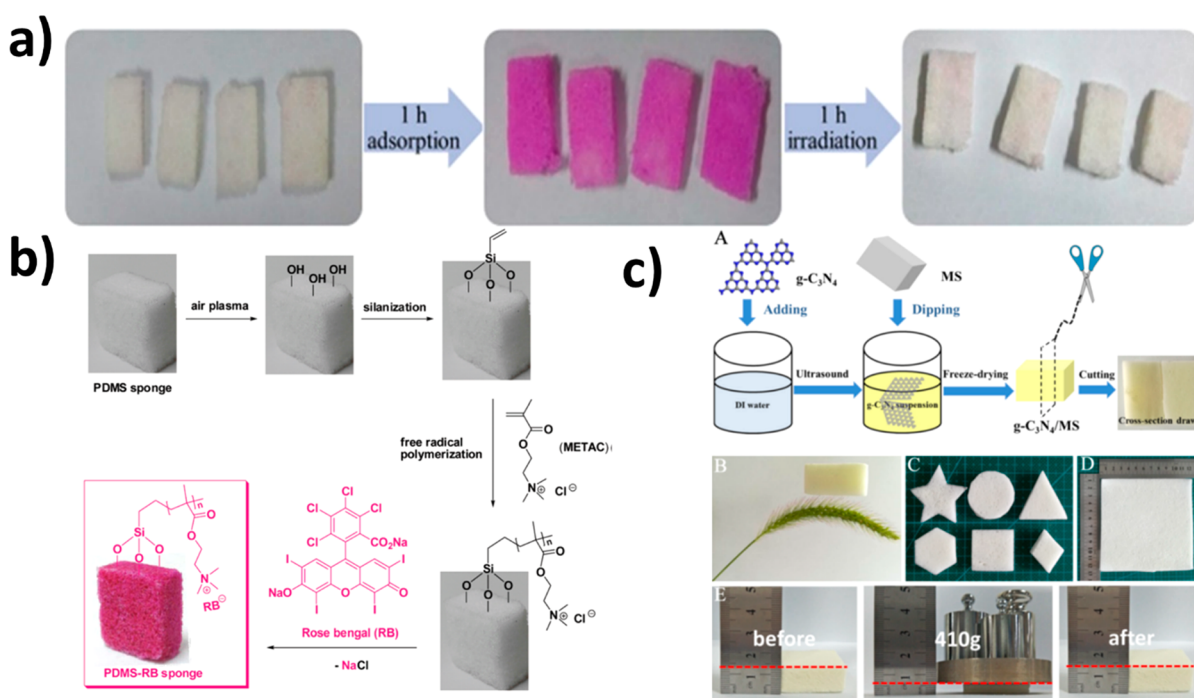


Figure 4. (a) Visible-light-induced self-cleaning activity of g-CN-based PDMS sponge visualized via photocatalytic RhB degradation [adapted from ref 115, published under ACS AuthorChoice, copyright 2020, American Chemical Society, Washington, DC]. (b) Formation of rose Bengal (RB)-grafted photocatalytic PDMS sponge [adapted with permission from ref 116, copyright 2017, Royal Society of Chemistry, London]. (c) Schematic description of the fabrication of g-CN-based photoactive melamine sponge, as well as digital images of various samples and a preliminary compression strength demonstration [obtained from ref 118, published under CC-BY distribution, copyright 2018, Frontiers Media].

synthesized via a sugar templating method (kneaded sugar particles mixed with different concentration of ZnO, immersed in PDMS prepolymer, cured and purified from sugar, respectively) resulted in 3D interconnected photoactive macroporous network. ZnO particles on PDMS matrix demonstrated excellent MB dye photodegradation under various light sources (UV, visible, and UV–visible). Strong adhesion of incorporated ZnO particles on the PDMS substrate was cross-checked via filtration methods to prosecute leached amounts of ZnO after the sugar-dissolving step.¹¹⁴ As an alternative to ZnO, ultrathin carbon nitride nanosheets (prepared via thermal condensation of melamine) decorated on PDMS sponge via injection also showed high photocatalytic activity according to performed RhB dye photodegradation results (PDMS sponge synthesized via a sugar template method, injected with CN nanosheets dispersion, as-prepared composite annealed at 200 °C for 2 h). Moreover, the photocatalyst composite exhibited selective absorption against various oils, self-cleaning feature (Figure 4a), separation of oil-in-water emulsion in biphasic system, and facile recyclability.¹¹⁵ However, there was no investigation on the stability or leaching of CN nanosheets. Overall, for embedding photocatalysts in PDMS matrix, the main consideration should be the accessibility of semiconductor particles. Even though porous structures are obtained, the location of semiconductors at the interface plays a key role in photocatalytic performances.

Surface modification of PDMS also can bring photoactivity. Therefore, it is certainly worth mentioning about surface post-modified PDMS photocatalysts showing unique performance in cross-dehydrogenative coupling (CDC) reactions via visible light. For example, rose bengal (RB) is immobilized on plasma-oxidized PDMS surface rich in hydroxyl groups (Figure 4b). Vinyltrimethoxysilane (VTMS) is used for silanization of

hydroxyl groups and resulting brushes polymerized via free-radical polymerization with 2-(methacryloyloxy)ethyl-trimethylammonium-chloride (METAC), and then mixed with RB disodium salt for ion exchange. Obtained PDMS-RB photocatalyst was examined in CDC reaction (*N*-phenyl tetrahydroisoquinoline-nitromethane) under visible-light illumination and results revealed its high efficiency which is almost comparable to the iridium (Ir)-based catalysts that are common for CDC reactions. Moreover, an easy-to-build continuous flow reactor setup demonstrates the industrial potential of the PDMS-RB sponge catalyst, and the results clearly indicate that a gram-scale reaction of CDC is very beneficial in flow reactor too (isolated yield 88% after 48 h).¹¹⁶ CDC of tertiary amines with ketones was succeeded via organic photoactive PDMS material. Plasma-treated hydroxy-rich PDMS sponge was modified with 3-aminopropyl trimethoxysilane and resulting amino groups were coupled with Fmoc-Glu(OtBu)–OH resulting in Glu-functionalized PDMS sponge. The PDMS-based photocatalyst offers a profitable solid-phase peptide synthesis (SPPS), which furthermore functions quite well for CDC reactions.¹¹⁷ These methods are constructed on covalent attachment of photoactive moieties, which is reported to result in enhanced photocatalytic performances. Yet, the active sides are restricted to modified surfaces rather than porous interfaces.

In addition to PDMS as a host network, melamine sponge (MS) is also an attractive choice, because it has high porosity, low density, good elasticity, amphiphilicity, low price, and industrial availability. For instance, MS was dipped into graphitic carbon nitride (g-C₃N₄) suspension, then squeezed and reimmersed until obtaining adequate amount of g-C₃N₄ over MS network, then freeze-dried to gain monolithic g-C₃N₄/MS (Figure 4c). This novel photoactive composite has

shown decent photooxidation ability according to NO photoremoval experiment (optimum activity = 78.6%) besides effective CO₂ photoreduction in comparison to powder g-C₃N₄.¹¹⁸ This is a post-embedding technique yet the potential leaching of g-CN particles should be investigated in detail.

In another study, significant photodegradation activity as well as excellent recyclability toward RhB dye under visible-light irradiation was achieved by carbon nitride foam (CNF)-supported hybrid photocatalyst (CNB). MS was initially carbonized via tube furnace and resulting CNF was dipped into BiOBr solution (Bi(NO₃)₃·5H₂O-CTAB in 40 mL of ethylene glycol) of different concentrations then placed in an autoclave (160 °C–16 h) in order to obtain hybrid CNF-supported BiOBr (CNB). This solvothermal photocatalyst fabrication method is a significant example for effective heterojunction between well-distributed BiOBr microspheres over fibrillar g-C₃N₄ scaffolds. In addition, the resulting low-density open macroporous structure granted floatability.¹¹⁹ In this case, authors transformed melamine sponge to a carbon nitride matrix, where it hosted another semiconductor to form heterojunctions.

Considering sponge-like features, a biomass source called “loofah” and its as-prepared sponge (derived from loofah plants) revealed unique properties to be applied as a biocarrier for an intimately coupled photocatalysis and biodegradation (ICPB) system. This natural macroporous structure is quite similar to synthetic sponges and, thus, can highlight the potential of biobased resources as porous networks. Combination of bio-sourced sponge with Bi₂₄O₃₁Br₁₀ photocatalyst, that was spray-coated, showed better performance than polyurethane-based competitive carriers (after being immersed in sludge) in the removal and mineralization of tetracycline hydrochloride (TCH) under visible light. The ICPB system works via the combination of photocatalysis and bacterial enzymatic degradation, so diffusion-based accessibility has prime importance. Under light irradiation, photoformed products (reactive oxygen species, ROS) successfully accessed the interior of the carrier and is biodegraded by the loaded amount of bacteria.¹²⁰

In a more-sophisticated way of utilizing sponge-like carriers, carbonized charred wood slices resulting in wood/photocatalyst (wood/CoO) architectures exhibited a high hydrogen production rate (up to 220.74 μmol h⁻¹ cm⁻²) under solar light. Photothermal–photocatalytic biphasic system prepared via spin coating of various photocatalyst dispersions (MoS₂, C₃N₄, TiO₂) homogeneously on the surface of carbonized wood slices pointed out that the carbonization of biobased resources as sponge-like host materials for photocatalysts can convert liquid water to water steam under solar light (Table 3).¹²¹ Yet spray coating semiconductors on porous surfaces strictly limits the allocation of photocatalyst to surface, which is why surface-driven photocatalytic reactions are entailed. It is also very important to identify stability against solvent leaching of coated structures to determine lifetime of composites.

RESINS

Resins are naturally occurring (plant based) or industrially produced (synthetic) robust organic matters. Their transformation to light-responsive structures after suitable combination with photoactive substances paves the way for highly effective hybrid materials for photobased applications. A good example for this, Novolac-type resin (PR, formaldehyde:phenol <1) generates surface complexation with TiO₂ particles

Table 3. Summary of Fabrication Methods for Photoactive Sponge–Foam Systems

references	fabrication method
109, 113, 114	Semiconductors are introduced during sol–gel process through dispersion
110–112, 115	introducing semiconducting particles to the cured PDMS sponge
116, 117	covalent modification of PDMS surface with organic photocatalysts
118	coating melamine sponge with semiconductor via immersing melamine sponge in semiconductor dispersion
119	coating semiconductor on carbonized melamine sponge through solvothermal process
120	spray coating semiconductor on loofah sponge
121	spin coating semiconductor dispersion onto carbonized wood

resulting in PR-complexed-TiO₂ composite, which shows very efficient photocatalytic H₂ evolution along with adequate photocurrent generation and favorable degradation of organic pollutants under visible-light irradiation.¹²² In the case of this, photoactivity relied on ligand-to-metal charge transfer (LMCT) sensitization, which occurred between adsorbate and TiO₂ particles through electron transfer process and most favorable PR-TiO₂ composite obtained via optimizing employed TiO₂ ratio. In another study with phenolic type resin, photosensitization was achieved via chlorophyll incorporation through Fisher esterification.¹²³ Chlorophyll-sensitized resin demonstrated favorable photoreduction mechanism via trapping charge carriers over chlorophyll (based on centered Mg ions) followed by electron flux throughout the phenolic resin based on electron delocalization property. In this way of integration, immobilization of chlorophyll on phenolic resin matrix provided higher photocatalytic activity besides superior chemical resistivity both in acidic and alkaline media simulated for photodegradation of the blue waste and MB. The starting point for these systems is the synthesis of phenolic resin matrix (i.e., phenol–formaldehyde) via polyaddition. Styrene-based vinyl containing resin matrices are popular choices as well. Copolymerization of styrene with photoactive 2,1,3-benzothiadiazole-based custom-made divinyl cross-linker via free-radical polymerization resulted in various heterogeneous photosensitizers in different forms (bead, monolith) (Figure 5a).¹²⁴ Resulting photoactive resin materials could form singlet oxygen species under visible-light irradiation that can be exploited for oxidative organic reactions. Furthermore, versatility of obtained forms showed different photocatalytic activities in batch and flow conditions, thanks to structural variability of resin matrix. Utilization of a side-chain conjugated polystyrene-based macroporous resin (tailor-made sulfamide-PS resin synthesized from chlorosulfonated PS resin) that is grafted with silver nanoparticles (Ag NPs) via sulfamide bonds successfully prevented common Ag NPs aggregation, thus the hybrid material exhibited excellent photocatalytic activity according to photoreduction reaction under visible light (from 4-nitrophenol (4-NP) to 4-aminophenol (4-AP)).¹²⁵

Alternatively, semiconductors can be integrated into resins during heterophase polymerization stage via dispersing semiconductors in organic monomer phase. For example, metal-free semiconductor (graphitic carbon nitride, g-CN, post-modified to bring organodispersibility) was dispersed in organic phase and its photoactivity was harvested by conducting suspension photopolymerization (Figure 5b).¹²⁶ In this case, polystyrene-

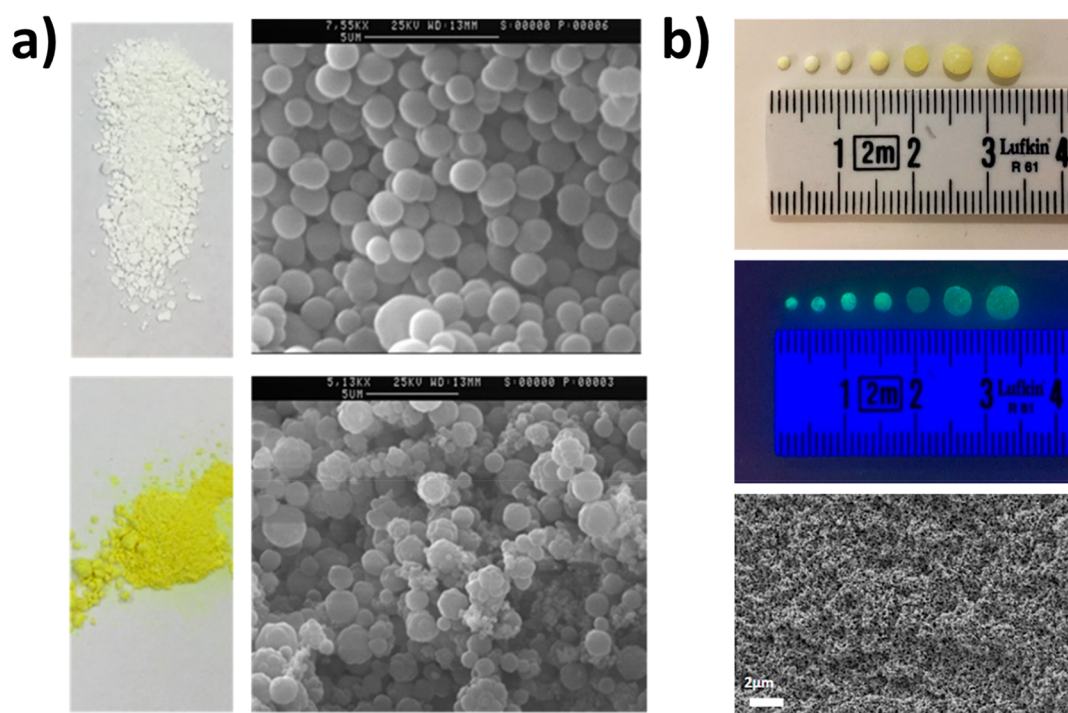


Figure 5. (a) Digital images and corresponding SEM images of reference beads (top) and beads containing photoactive groups (below) [adapted with permission from ref 124, copyright 2017, American Chemical Society, Washington, DC]. (b) Digital images of g-CN based PS-DVB beads under normal and UV light, and an exemplary SEM image of a bead showing a porous network [obtained from ref 126, published under CC-BY, copyright 2021, John Wiley and Sons].

divinylbenzene (PS-DVB) beads were upgraded into a photoactive covalent porous hybrid resin where g-CN particles reside at the interface, which endows photoactivity confirmed via RhB dye photodegradation experiments. As a last example, thiol–ene polymer beads will be discussed. Multifunctional thiol–ene molecules in carbon nitride organic dispersion can be injected into aqueous boric acid solution to afford stable bead shapes due to liquid–liquid printing based on interfacial jamming of oppositely charged molecules. Applying UV light initiates polymerization via g-CN and g-CN remains solely on the surface of macroscale beads. The process is prone to scale up and automation, yet resulting beads were not photoactive as porosity is blocked by g-CN nanosheets on surface. This highlights the importance of light and solvent accessible porosity as a key driving factor to achieve functioning photoactive composites (Table 4).¹²⁷

CONCLUSIONS

When one hunts a structural stability against solvent, temperature, pH, etc., cross-linked polymer networks can offer desirable properties. Over 100 years of polymer science, some of the industrial processes that benefit humankind rely on the utilization of cross-linked polymer systems. Herein, we

provide an alternative perspective on such materials by peering into their photoactive properties, thanks to semiconductor incorporation. That is a mutual benefit for both materials, because semiconductors then can be scaled up to a macroscale with dimensional stability. We featured aqueous hydrogels, aerogels-organogels, silicon-based PDMS and organic resin materials as host networks, and we have summarized how the literature, until now, has dealt with attaching photoactivity. Semiconductors can be incorporated through embedding, or their photoactivity can be already harnessed at an initial stage to form covalent hybrids. Porosity is a key feature to possess in order to maximize semiconductor–light contact. It is important to note that the photocatalytic activity of composites is generally less than that of pure photocatalyst powders, yet use active scaffolds, which can induce charge separation processes and surpasses such problems. Careful readers might realize the lack of photocatalytic performance of composites by numbers in this Review. While powder photocatalyst performances are reported per gram or milligram of powder employed, for composite structures it becomes really challenging. First, experiments are targeted for macroscale applications, and, as a result, employed scales are large; and the amount of photocatalyst, location of photocatalyst, porosity and scaffold type have major influence on performances. Hence, it is not a fair judgment when photoactivities by means of numbers are compared in this case. Porous polymers promoted with photoactivity are extremely attractive for scaled-up heterogeneous photocatalysis, environmental remediation, and tailored organic synthesis.

PERSPECTIVES AND FUTURE ASPECTS

Even though the research in this direction currently in its infant stage, a future with great possibilities awaits. Enhancing

Table 4. Summary of Fabrication Methods for Photoactive Resin Systems

reference(s)	fabrication method
122	surface complexation
123	covalent chlorophyll attachment
124	photoactive unit is part of cross-linker
125	surface grafting of photocatalyst to resin
126, 127	covalent polymer initiation from semiconductor surface

solid content of semiconductors in corresponding polymer networks can result in improved photoactivities. Searching for sustainable monomers to form the skeleton of photoactive porous polymers is a must. Alternative network formations, for example via thiol–ene and azide–alkyne based, can be explored. The importance of automated and/or flow synthesis and optimization of parameters via artificial intelligence (AI) must be governed. Formation of ternary composites by surface doping (i.e., insertion of metals) might significantly enhance overall photocatalytic activities. Application border of photoactive composites can be pushed forward to encapsulate trends such as biomass conversion, energy generation and storage, photoinduced synthesis of H₂ fuel, etc. Modern manufacturing methods to form macroscale hybrids must be investigated. It is important to provide a life cycle assessment and identify possible recycling routes for photoactive cross-linked polymers to avoid landfilling and waste formation. To conclude, the future is full of opportunities for semiconductor incorporated polymer networks and so-formed photoactive hybrid materials will pioneer industrial transformation.

AUTHOR INFORMATION

Corresponding Author

Baris Kumru – *Aerospace Structures and Materials Department, Faculty of Aerospace Engineering, Delft University of Technology, 2629 HS Delft, The Netherlands;*
orcid.org/0000-0002-1203-4019; Email: b.kumru@tudelft.nl

Author

Cansu Esen – *Department of Colloid Chemistry, Max Planck Institute of Colloids and Interfaces, 14476 Potsdam, Germany*

Complete contact information is available at:
<https://pubs.acs.org/10.1021/acs.iecr.2c01658>

Notes

The authors declare no competing financial interest.

REFERENCES

- (1) Scott, T. F.; Schneider, A. D.; Cook, W. D.; Bowman, C. N. Photoinduced Plasticity in Cross-Linked Polymers. *Science* **2005**, *308* (5728), 1615–1617.
- (2) Yanagisawa, Y.; Nan, Y.; Okuro, K.; Aida, T. Mechanically robust, readily repairable polymers via tailored noncovalent cross-linking. *Science* **2018**, *359* (6371), 72–76.
- (3) Yu, S.; Zhang, R.; Wu, Q.; Chen, T.; Sun, P. Bio-Inspired High-Performance and Recyclable Cross-Linked Polymers. *Adv. Mater.* **2013**, *25* (35), 4912–4917.
- (4) Fortman, D. J.; Brutman, J. P.; De Hoe, G. X.; Snyder, R. L.; Dichtel, W. R.; Hillmyer, M. A. Approaches to Sustainable and Continually Recyclable Cross-Linked Polymers. *ACS Sustainable Chem. Eng.* **2018**, *6* (9), 11145–11159.
- (5) Kloxin, C. J.; Scott, T. F.; Adzima, B. J.; Bowman, C. N. Covalent Adaptable Networks (CANs): A Unique Paradigm in Cross-Linked Polymers. *Macromolecules* **2010**, *43* (6), 2643–2653.
- (6) Chen, J.; Garcia, E. S.; Zimmerman, S. C. Intramolecularly Cross-Linked Polymers: From Structure to Function with Applications as Artificial Antibodies and Artificial Enzymes. *Acc. Chem. Res.* **2020**, *53* (6), 1244–1256.
- (7) Kumru, B.; Molinari, V.; Hilgart, M.; Rummel, F.; Schaeffler, M.; Schmidt, B. V. K. J. Polymer Grafted Graphitic Carbon Nitride as Precursors for Reinforced Lubricant Hydrogels. *Poly Chem.* **2019**, *10*, 3647–3656.
- (8) Ozer, O.; Ince, A.; Karagoz, B.; Bicak, N. Crosslinked PS-DVB microspheres with sulfonated polystyrene brushes as new generation of ion exchange resins. *Desalination* **2013**, *309*, 141–147.
- (9) Liu, M.; Ishida, Y.; Ebina, Y.; Sasaki, T.; Hikima, T.; Takata, M.; Aida, T. An anisotropic hydrogel with electrostatic repulsion between cofacially aligned nanosheets. *Nature* **2015**, *517* (7532), 68–72.
- (10) Nguyen, K. D. Q.; Crespo-Ribadeneyra, M.; Picot, O.; Colak, B.; Gautrot, J. E. Ultrafast Photo-Crosslinking of Thiol-Norbornene Opaque Silicone Elastomer Nanocomposites in Air. *ACS Appl. Poly Mater.* **2021**, *3* (11), 5373–5385.
- (11) Fernández-Francos, X.; Ramis, X. Structural analysis of the curing of epoxy thermosets crosslinked with hyperbranched poly(ethyleneimine)s. *Eur. Polym. J.* **2015**, *70*, 286–305.
- (12) Rahman, N. S. A.; Ahmad, N. A.; Yhaya, M. F.; Azahari, B.; Ismail, W. R. Crosslinking of fibers via azide-alkyne click chemistry: Synthesis and characterization. *J. Appl. Polym. Sci.* **2016**, *133* (25), 43576.
- (13) Wang, Y.; Chen, Q.; Chen, M.; Guan, Y.; Zhang, Y. PHEMA hydrogel films crosslinked with dynamic disulfide bonds: synthesis, swelling-induced mechanical instability and self-healing. *Poly Chem.* **2019**, *10* (35), 4844–4851.
- (14) Mondal, P.; Saha, S. K.; Chowdhury, P. Simultaneous polymerization and quaternization of 4-vinyl pyridine. *J. Appl. Polym. Sci.* **2013**, *127* (6), 5045–5050.
- (15) Wang, Y. J.; Zhang, X. N.; Song, Y.; Zhao, Y.; Chen, L.; Su, F.; Li, L.; Wu, Z. L.; Zheng, Q. Ultrastiff and Tough Supramolecular Hydrogels with a Dense and Robust Hydrogen Bond Network. *Chem. Mater.* **2019**, *31* (4), 1430–1440.
- (16) Le, X. T.; Turgeon, S. L. Rheological and structural study of electrostatic cross-linked xanthan gum hydrogels induced by β -lactoglobulin. *Soft Matter* **2013**, *9* (11), 3063–3073.
- (17) Chen, T.; Li, M.; Liu, J. π - π Stacking Interaction: A Nondestructive and Facile Means in Material Engineering for Bioapplications. *Cryst. Growth Des.* **2018**, *18* (5), 2765–2783.
- (18) Li, T.; Kumru, B.; Al Nakeeb, N.; Willersinn, J.; Schmidt, B. V. K. J. Thermoadaptive Supramolecular α -Cyclodextrin Crystallization-Based Hydrogels via Double Hydrophilic Block Copolymer Templating. *Polymers* **2018**, *10* (6), 576.
- (19) Appel, E. A.; Biedermann, F.; Rauwald, U.; Jones, S. T.; Zayed, J. M.; Scherman, O. A. Supramolecular Cross-Linked Networks via Host-Guest Complexation with Cucurbit[8]uril. *J. Am. Chem. Soc.* **2010**, *132* (40), 14251–14260.
- (20) Kumru, B.; Molinari, V.; Dunnebacke, R.; Blank, K. G.; Schmidt, B. V. K. J. Extremely Compressible Hydrogel via Incorporation of Modified Graphitic Carbon Nitride. *Macromol. Rapid Commun.* **2019**, *40* (4), 1800712.
- (21) Parhi, R. Cross-Linked Hydrogel for Pharmaceutical Applications: A Review. *Adv. Pharm. Bull.* **2017**, *7* (4), 515–530.
- (22) Liu, Q.; Yan, K.; Chen, J.; Xia, M.; Li, M.; Liu, K.; Wang, D.; Wu, C.; Xie, Y. Recent advances in novel aerogels through the hybrid aggregation of inorganic nanomaterials and polymeric fibers for thermal insulation. *Aggregate* **2021**, *2* (2), No. e30.
- (23) Kumru, B.; Gure, B.; Bicak, N. Regio-selective peroxybromination of poly(vinyl methyl ketone) as versatile tool for generation active ATRP initiation sites on solid surfaces. *J. Polym. Sci., Part A: Polym. Chem.* **2013**, *51* (18), 3892–3900.
- (24) Zeng, L.; Lin, X.; Li, P.; Liu, F.-Q.; Guo, H.; Li, W.-H. Recent advances of organogels: from fabrications and functions to applications. *Prog. Org. Coat.* **2021**, *159*, 106417.
- (25) Zhu, D.; Handschuh-Wang, S.; Zhou, X. Recent progress in fabrication and application of polydimethylsiloxane sponges. *J. Mater. Chem. A* **2017**, *5* (32), 16467–16497.
- (26) Spicer, C. D. Hydrogel scaffolds for tissue engineering: the importance of polymer choice. *Poly Chem.* **2020**, *11* (2), 184–219.
- (27) Liang, Y.; He, J.; Guo, B. Functional Hydrogels as Wound Dressing to Enhance Wound Healing. *ACS Nano* **2021**, *15* (8), 12687–12722.
- (28) Tsai, P.-L.; Sung, T.-Y.; Chong, C.-Y.; Huang, S.-Y.; Chen, S.-F. Comparison of poly(styrene-divinylbenzene)-based monolithic and

- bead-based methodologies used in NANOFLOW LCMS for proteomic studies. *Anal. Methods* **2018**, *10* (39), 4756–4764.
- (29) Suriboot, J.; Bazzi, H. S.; Bergbreiter, D. E. Supported Catalysts Useful in Ring-Closing Metathesis, Cross Metathesis, and Ring-Opening Metathesis Polymerization. *Polymers* **2016**, *8* (4), 140.
- (30) Xiao, Y.; Li, L.; Zhang, S.; Feng, J.; Jiang, Y.; Feng, J. Thermal Insulation Characteristics of Polybenzoxazine Aerogels. *Macromol. Mater. Eng.* **2019**, *304* (7), 1900137.
- (31) Lim, H. W.; Lee, S. J. Double-insulated porous PDMS sponge for heat-localized solar evaporative seawater desalination. *Desalination* **2022**, *526*, 115540.
- (32) Zhang, J. Z.; Reisner, E. Advancing photosystem II photoelectrochemistry for semi-artificial photosynthesis. *Nature Reviews Chemistry* **2020**, *4* (1), 6–21.
- (33) Kärkäs, M. D.; Verho, O.; Johnston, E. V.; Åkermark, B. Artificial Photosynthesis: Molecular Systems for Catalytic Water Oxidation. *Chem. Rev.* **2014**, *114* (24), 11863–12001.
- (34) Zhang, B.; Sun, L. Artificial photosynthesis: opportunities and challenges of molecular catalysts. *Chem. Soc. Rev.* **2019**, *48* (7), 2216–2264.
- (35) Chhowalla, M.; Jena, D.; Zhang, H. Two-dimensional semiconductors for transistors. *Nat. Rev. Mater.* **2016**, *1*, 16052.
- (36) Wang, C.; Dong, H.; Jiang, L.; Hu, W. Organic semiconductor crystals. *Chem. Soc. Rev.* **2018**, *47* (2), 422–500.
- (37) Fujishima, A.; Honda, K. Electrochemical Photolysis of Water at a Semiconductor Electrode. *Nature* **1972**, *238*, 37–38.
- (38) Kándóth, N.; Hernandez, J. P.; Palomares, E.; Lloret-Fillol, J. Mechanisms of photoredox catalysts: the role of optical spectroscopy. *Sustain. Energy Fuels* **2021**, *5* (3), 638–665.
- (39) Corrigan, N.; Shanmugam, S.; Xu, J.; Boyer, C. Photocatalysis in organic and polymer synthesis. *Chem. Soc. Rev.* **2016**, *45* (22), 6165–6212.
- (40) Mazzanti, S.; Manfredi, G.; Barker, A. J.; Antonietti, M.; Savateev, A.; Giusto, P. Carbon Nitride Thin Films as All-In-One Technology for Photocatalysis. *ACS Catal.* **2021**, *11*, 11109–11116.
- (41) Mazzanti, S.; Savateev, A. Emerging Concepts in Carbon Nitride Organic Photocatalysis. *ChemPlusChem.* **2020**, *85* (11), 2499–2517.
- (42) Teranishi, T.; Sakamoto, M. Charge Separation in Type-II Semiconductor Heterodimers. *J. Phys. Chem. Lett.* **2013**, *4* (17), 2867–2873.
- (43) Chen, F.; Ma, T.; Zhang, T.; Zhang, Y.; Huang, H. Atomic-Level Charge Separation Strategies in Semiconductor-Based Photocatalysts. *Adv. Mater.* **2021**, *33* (10), 2005256.
- (44) Sundin, E.; Abrahamsson, M. Long-lived charge separation in dye-semiconductor assemblies: A pathway to multi-electron transfer reactions. *Chem. Commun.* **2018**, *54* (42), 5289–5298.
- (45) Xia, J.; Mark, G.; Volokh, M.; Fang, Y.; Chen, H.; Wang, X.; Shalom, M. Supramolecular organization of melem for the synthesis of photoactive porous carbon nitride rods. *Nanoscale* **2021**, *13* (46), 19511–19517.
- (46) Karjule, N.; Phatake, R.; Volokh, M.; Hod, I.; Shalom, M. Solution-Processable Carbon Nitride Polymers for Photoelectrochemical Applications. *Small Methods* **2019**, *3* (12), 1900401.
- (47) Barrio, J.; Shalom, M. Rational Design of Carbon Nitride Materials by Supramolecular Preorganization of Monomers. *ChemCatChem.* **2018**, *10* (24), 5573–5586.
- (48) Zhang, J.; Antonietti, M.; Kumru, B. Colloidal Tornadoes in a Vial under Gravitational Sedimentation. *J. Chem. Educ.* **2021**, *98* (4), 1347–1351.
- (49) Jin, L.; Zhao, H.; Wang, Z. M.; Rosei, F. Quantum Dots-Based Photoelectrochemical Hydrogen Evolution from Water Splitting. *Adv. Energy Mater.* **2021**, *11* (12), 2003233.
- (50) Villa, K.; Galan-Mascaros, J. R.; Lopez, N.; Palomares, E. Photocatalytic water splitting: advantages and challenges. *Sustain. Energy Fuels* **2021**, *5* (18), 4560–4569.
- (51) Bian, H.; Li, D.; Yan, J.; Liu, S. F. Perovskite—A wonder catalyst for solar hydrogen production. *J. Energy Chem.* **2021**, *57*, 325–340.
- (52) Shaw, M. H.; Twilton, J.; MacMillan, D. W. C. Photoredox Catalysis in Organic Chemistry. *J. Org. Chem.* **2016**, *81* (16), 6898–6926.
- (53) Romero, N. A.; Nicewicz, D. A. Organic Photoredox Catalysis. *Chem. Rev.* **2016**, *116* (17), 10075–10166.
- (54) Jena, A. K.; Kulkarni, A.; Miyasaka, T. Halide Perovskite Photovoltaics: Background, Status, and Future Prospects. *Chem. Rev.* **2019**, *119* (5), 3036–3103.
- (55) Avrutin, V.; Izyumskaya, N.; Morkoc, H. Semiconductor solar cells: Recent progress in terrestrial applications. *Superlattices Microstruct.* **2011**, *49* (4), 337–364.
- (56) Byrne, C.; Subramanian, G.; Pillai, S. C. Recent advances in photocatalysis for environmental applications. *J. Environ. Chem. Eng.* **2018**, *6* (3), 3531–3555.
- (57) Marszewski, M.; Cao, S.; Yu, J.; Jaroniec, M. Semiconductor-based photocatalytic CO₂ conversion. *Mater. Horiz.* **2015**, *2* (3), 261–278.
- (58) Kumru, B.; Cruz, D.; Heil, T.; Antonietti, M. In Situ Formation of Arrays of Tungsten Single Atoms within Carbon Nitride Frameworks Fabricated by One-Step Synthesis through Monomer Complexation. *Chem. Mater.* **2020**, *32* (21), 9435–9443.
- (59) Kaya, K.; Kiskan, B.; Kumru, B.; Schmidt, B. V. K. J.; Yagci, Y. An oxygen-tolerant visible light induced free radical polymerization using mesoporous graphitic carbon nitride. *Eur. Polym. J.* **2020**, *122*, 109410.
- (60) Buz, E.; Morlet-Savary, F.; Lalevé, J.; Acar, H. Y. CdS-Oleic Acid Quantum Dots as Long-Wavelength Photoinitiators in Organic Solvent and Preparation of Luminescent, Colloidal CdS/Polymer Nanocomposites. *Macromol. Chem. Phys.* **2018**, *219* (2), 1700356.
- (61) Kim, J.-H.; Seo, S.; Lee, J.-H.; Choi, H.; Kim, S.; Piao, S.; Kim, Y. R.; Park, B.; Lee, J.; Jung, Y.; Park, H.; Lee, S.; Lee, K. Efficient and Stable Perovskite-Based Photocathode for Photoelectrochemical Hydrogen Production. *Adv. Funct. Mater.* **2021**, *31* (17), 2008277.
- (62) Tashakory, A.; Karjule, N.; Abisdris, L.; Volokh, M.; Shalom, M. Mediated Growth of Carbon Nitride Films via Spray-Coated Seeding Layers for Photoelectrochemical Applications. *Adv. Sustain. Syst.* **2021**, *5* (11), 2100005.
- (63) Coperet, C.; Chabanas, M.; Saint-Arroman, R. P.; Basset, J.-M. Homogeneous and Heterogeneous Catalysis: Bridging the Gap through Surface Organometallic Chemistry. *Angew. Chem. Int. Ed.* **2003**, *42* (2), 156–181.
- (64) Kumru, B.; Antonietti, M. Colloidal properties of the metal-free semiconductor graphitic carbon nitride. *Adv. Colloid Interface Sci.* **2020**, *283*, 102229.
- (65) Kumru, B.; Barrio, J.; Zhang, J.; Antonietti, M.; Shalom, M.; Schmidt, B. V. K. J. Robust Carbon Nitride-Based Thermoset Coatings for Surface Modification and Photochemistry. *ACS Appl. Mater. Interfaces* **2019**, *11* (9), 9462–9469.
- (66) Thurston, J. H.; Clifford, A. J.; Henderson, B. S.; Smith, T. R.; Quintana, D.; Cudworth, K. F.; Lujan, T. J.; Cornell, K. A. Development of Photoactive g-C₃N₄/Poly(vinyl alcohol) Composite Hydrogel Films with Antimicrobial and Antibiofilm Activity. *ACS Appl. Bio Mater.* **2020**, *3* (3), 1681–1689.
- (67) Chen, M.; Cui, Z.; Edmondson, S.; Hodson, N.; Zhou, M.; Yan, J.; O'Brien, P.; Saunders, B. R. Photoactive composite films prepared from mixtures of polystyrene microgel dispersions and poly(3-hexylthiophene) solutions. *Soft Matter* **2015**, *11* (42), 8322–8332.
- (68) Chanklom, P.; Kreetachat, T.; Chotigawin, R.; Suwannahong, K. Photocatalytic Oxidation of PLA/TiO₂-Composite Films for Indoor Air Purification. *ACS Omega* **2021**, *6* (16), 10629–10636.
- (69) Nicosia, A.; Vento, F.; Di Mari, G. M.; D'Urso, L.; Mineo, P. G. TiO₂-Based Nanocomposites Thin Film Having Boosted Photocatalytic Activity for Xenobiotics Water Pollution Remediation. *Nanomaterials* **2021**, *11* (2), 400.
- (70) Han, C.; Meng, P.; Waclawik, E. R.; Zhang, C.; Li, X.-H.; Yang, H.; Antonietti, M.; Xu, J. Palladium/Graphitic Carbon Nitride (g-C₃N₄) Stabilized Emulsion Microreactor as a Store for Hydrogen from Ammonia Borane for Use in Alkene Hydrogenation. *Angew. Chem. Int. Ed.* **2018**, *57* (45), 14857–14861.

- (71) Yandrapalli, N.; Robinson, T.; Antonietti, M.; Kumru, B. Graphitic Carbon Nitride Stabilizers Meet Microfluidics: From Stable Emulsions to Photoinduced Synthesis of Hollow Polymer Spheres. *Small* **2020**, *16* (32), 2001180.
- (72) Zhai, W.; Wu, Z.-M.; Wang, X.; Song, P.; He, Y.; Wang, R.-M. Preparation of epoxy-acrylate copolymer@nano-TiO₂ Pickering emulsion and its antibacterial activity. *Prog. Org. Coat.* **2015**, *87*, 122–128.
- (73) Lee, S.-J.; Choi, J. W.; Kumar, S.; Lee, C.-L.; Lee, J.-S. Preparation of perovskite-embedded monodisperse copolymer particles and their application for high purity down-conversion LEDs. *Mater. Horiz* **2018**, *5* (6), 1120–1129.
- (74) Gunaratne, H. Q. N.; Pestana, C. J.; Skillen, N.; Hui, J.; Saravanan, S.; Edwards, C.; Irvine, J. T. S.; Robertson, P. K. J.; Lawton, L. A. 'All in one' photo-reactor pod containing TiO₂ coated glass beads and LEDs for continuous photocatalytic destruction of cyanotoxins in water. *Environ. Sci. Water Res. Technol.* **2020**, *6* (4), 945–950.
- (75) Zhang, S.; Zhang, J.; Sun, J.; Tang, Z. Capillary micro-photoreactor packed with TiO₂-coated glass beads: An efficient tool for photocatalytic reaction. *Chem. Eng. Process* **2020**, *147*, 107746.
- (76) Bell, K.; Freeburne, S.; Fromel, M.; Oh, H. J.; Pester, C. W. Heterogeneous photoredox catalysis using fluorescein polymer brush functionalized glass beads. *J. Polym. Sci.* **2021**, *59*, 2844–2853.
- (77) Bansal, P.; Verma, A. Synergistic effect of dual process (photocatalysis and photo-Fenton) for the degradation of Cephalexin using TiO₂ immobilized novel clay beads with waste fly ash/foundry sand. *J. Photochem. Photobiol. A* **2017**, *342*, 131–142.
- (78) Dallabona, I. D.; Mathias, A. L.; Jorge, R. M. M. A new green floating photocatalyst with Brazilian bentonite into TiO₂/alginate beads for dye removal. *Colloids Surf. A* **2021**, *627*, 127159.
- (79) Li, D.; Zhu, Q.; Han, C.; Yang, Y.; Jiang, W.; Zhang, Z. Photocatalytic degradation of recalcitrant organic pollutants in water using a novel cylindrical multi-column photoreactor packed with TiO₂-coated silica gel beads. *J. Hazard Mater.* **2015**, *285*, 398–408.
- (80) Spagnul, C.; Greenman, J.; Wainwright, M.; Kamil, Z.; Boyle, R. W. Synthesis, characterization and biological evaluation of a new photoactive hydrogel against Gram-positive and Gram-negative bacteria. *J. Mater. Chem. B* **2016**, *4* (8), 1499–1509.
- (81) Lei, W.; Suzuki, N.; Terashima, C.; Fujishima, A. Hydrogel photocatalysts for efficient energy conversion and environmental treatment. *Front Energy* **2021**, *15* (3), 577–595.
- (82) Ma, Y.; Wang, J.; Xu, S.; Zheng, Z.; Du, J.; Feng, S.; Wang, J. Ag₂O/sodium alginate supramolecular hydrogel as a film photocatalyst for removal of organic dyes in wastewater. *RSC Adv.* **2017**, *7* (25), 15077–15083.
- (83) Mai, N. X. D.; Bae, J.; Kim, I. T.; Park, S. H.; Lee, G.-W.; Kim, J. H.; Lee, D.; Son, H. B.; Lee, Y.-C.; Hur, J. A recyclable, recoverable, and reformable hydrogel-based smart photocatalyst. *Environ. Sci. Nano* **2017**, *4* (4), 955–966.
- (84) You, X.; Huang, H.; Zhang, R.; Yang, Z.; Xu, M.; Wang, X.; Yao, Y. Immobilization of TiO₂ Nanoparticles in Hydrogels Based on Poly(methyl acrylate) and Succinamide Acid for the Photo-degradation of Organic Dyes. *Catalysts* **2021**, *11* (5), 613.
- (85) Sun, J.; Schmidt, B. V. K. J.; Wang, X.; Shalom, M. Self-Standing Carbon Nitride-Based Hydrogels with High Photocatalytic Activity. *ACS Appl. Mater. Interfaces* **2017**, *9* (3), 2029–2034.
- (86) Kumru, B.; Molinari, V.; Hilgart, M.; Rummel, F.; Schäffler, M.; Schmidt, B. V. K. J. Polymer grafted graphitic carbon nitrides as precursors for reinforced lubricant hydrogels. *Poly Chem.* **2019**, *10* (26), 3647–3656.
- (87) Cao, Q.; Barrio, J.; Antonietti, M.; Kumru, B.; Shalom, M.; Schmidt, B. V. K. J. Photoactive Graphitic Carbon Nitride-Based Gel Beads As Recyclable Photocatalysts. *ACS Appl. Poly Mater.* **2020**, *2* (8), 3346–3354.
- (88) Esen, C.; Kumru, B. Photoinduced post-modification of graphitic carbon nitride-embedded hydrogels: synthesis of 'hydrophobic hydrogels' and pore substructuring. *Beilstein J. Org. Chem.* **2021**, *17*, 1323–1334.
- (89) Fu, G.-B.; Xie, R.; Qin, J.-W.; Deng, X.-B.; Ju, X.-J.; Wang, W.; Liu, Z.; Chu, L.-Y. Facile Fabrication of Photocatalyst-Immobilized Gel Beads with Interconnected Macropores for the Efficient Removal of Pollutants in Water. *Ind. Eng. Chem. Res.* **2021**, *60* (24), 8762–8775.
- (90) Heidarpour, H.; Golizadeh, M.; Padervand, M.; Karimi, A.; Vossoughi, M.; Tavakoli, M. H. In-situ formation and entrapment of Ag/AgCl photocatalyst inside cross-linked carboxymethyl cellulose beads: A novel photoactive hydrogel for visible-light-induced photocatalysis. *J. Photochem. Photobiol. A* **2020**, *398*, 112559.
- (91) Yang, J.; Li, Z.; Zhu, H. Adsorption and photocatalytic degradation of sulfamethoxazole by a novel composite hydrogel with visible light irradiation. *Appl. Catal. B* **2017**, *217*, 603–614.
- (92) Zhu, H.; Li, Z.; Yang, J. A novel composite hydrogel for adsorption and photocatalytic degradation of bisphenol A by visible light irradiation. *Chem. Eng. J.* **2018**, *334*, 1679–1690.
- (93) Byun, J.; Landfester, K.; Zhang, K. A. I. Conjugated Polymer Hydrogel Photocatalysts with Expandable Photoactive Sites in Water. *Chem. Mater.* **2019**, *31* (9), 3381–3387.
- (94) Sai, H.; Erbas, A.; Dannenhoffer, A.; Huang, D.; Weingarten, A.; Siismets, E.; Jang, K.; Qu, K.; Palmer, L. C.; Olvera de la Cruz, M.; Stupp, S. I. Chromophore amphiphile-polyelectrolyte hybrid hydrogels for photocatalytic hydrogen production. *J. Mater. Chem. A* **2020**, *8* (1), 158–168.
- (95) Kuckhoff, T.; Landfester, K.; Zhang, K. A. I.; Ferguson, C. T. J. Photocatalytic Hydrogels with a High Transmission Polymer Network for Pollutant Remediation. *Chem. Mater.* **2021**, *33* (23), 9131–9138.
- (96) Gao, Y.; Gu, S.; Duan, L.; Wang, Y.; Gao, G. Robust and anti-fatigue hydrophobic association hydrogels assisted by titanium dioxide for photocatalytic activity. *Soft Matter* **2019**, *15* (19), 3897–3905.
- (97) Katzenberg, A.; Raman, A.; Schnabel, N. L.; Quispe, A. L.; Silverman, A. I.; Modestino, M. A. Photocatalytic hydrogels for removal of organic contaminants from aqueous solution in continuous flow reactors. *React. Chem. Eng.* **2020**, *5* (2), 377–386.
- (98) Liu, J.; Chen, H.; Shi, X.; Nawar, S.; Werner, J. G.; Huang, G.; Ye, M.; Weitz, D. A.; Solovev, A. A.; Mei, Y. Hydrogel microcapsules with photocatalytic nanoparticles for removal of organic pollutants. *Environ. Sci. Nano* **2020**, *7* (2), 656–664.
- (99) Ma, C.; Seo, W. C.; Lee, J.; Kim, Y.; Jung, H.; Yang, W. Construction of quantum dots self-decorated BiVO₄/reduced graphene hydrogel composite photocatalyst with improved photocatalytic performance for antibiotics degradation. *Chemosphere* **2021**, *275*, 130052.
- (100) Yong, Z.; Yap, L. W.; Fu, R.; Shi, Q.; Guo, Z.; Cheng, W. Seagrass-inspired design of soft photocatalytic sheets based on hydrogel-integrated free-standing 2D nanoassemblies of multifunctional nanohexagons. *Mater. Horiz.* **2021**, *8* (9), 2533–2540.
- (101) Zhang, H.; Zhou, L.; Li, J.; Rong, S.; Jiang, J.; Liu, S. Photocatalytic Degradation of Tetracycline by a Novel (CMC)/MIL-101(Fe)/β-CDP Composite Hydrogel. *Front Chem.* **2021**, *8*, 593730.
- (102) Wan, W.; Zhang, R.; Ma, M.; Zhou, Y. Monolithic aerogel photocatalysts: a review. *J. Mater. Chem. A* **2018**, *6* (3), 754–775.
- (103) Ou, H.; Yang, P.; Lin, L.; Anpo, M.; Wang, X. Carbon Nitride Aerogels for the Photoredox Conversion of Water. *Angew. Chem., Int. Ed.* **2017**, *56* (36), 10905–10910.
- (104) Mehmood, C. T.; Zhong, Z.; Zhou, H.; Zhang, C.; Xiao, Y. Immobilizing a visible light-responsive photocatalyst on a recyclable polymeric composite for floating and suspended applications in water treatment. *RSC Adv.* **2020**, *10* (60), 36349–36362.
- (105) Schreck, M.; Kleger, N.; Matter, F.; Kwon, J.; Tervoort, E.; Masania, K.; Studart, A. R.; Niederberger, M. 3D Printed Scaffolds for Monolithic Aerogel Photocatalysts with Complex Geometries. *Small* **2021**, *17* (50), 2104089.
- (106) Rizzo, C.; Marullo, S.; Billeci, F.; D'Anna, F. Catalysis in Supramolecular Systems: the Case of Gel Phases. *Eur. J. Org. Chem.* **2021**, *2021* (22), 3148–3169.
- (107) Chatterjee, S.; Kuppan, B.; Maitra, U. A self-assembled CdSe QD-organogel hybrid: photophysical and thermoresponsive properties. *Dalton Trans* **2018**, *47* (8), 2522–2530.

- (108) Sosnin, I. M.; Vlassov, S.; Dorogin, L. M. Application of polydimethylsiloxane in photocatalyst composite materials: A review. *React. Funct. Polym.* **2021**, *158*, 104781.
- (109) Deng, Z.-Y.; Wang, W.; Mao, L.-H.; Wang, C.-F.; Chen, S. Versatile superhydrophobic and photocatalytic films generated from TiO₂-SiO₂@PDMS and their applications on fabrics. *J. Mater. Chem. A* **2014**, *2* (12), 4178–4184.
- (110) Kim, D. H.; Jung, M. C.; Cho, S.-H.; Kim, S. H.; Kim, H.-Y.; Lee, H. J.; Oh, K. H.; Moon, M.-W. UV-responsive nano-sponge for oil absorption and desorption. *Sci. Rep* **2015**, *5* (1), 12908.
- (111) Hickman, R.; Walker, E.; Chowdhury, S. TiO₂-PDMS composite sponge for adsorption and solar mediated photo-degradation of dye pollutants. *J. Water Process Eng.* **2018**, *24*, 74–82.
- (112) Lee, S. Y.; Kang, D.; Jeong, S.; Do, H. T.; Kim, J. H. Photocatalytic Degradation of Rhodamine B Dye by TiO₂ and Gold Nanoparticles Supported on a Floating Porous Polydimethylsiloxane Sponge under Ultraviolet and Visible Light Irradiation. *ACS Omega* **2020**, *5* (8), 4233–4241.
- (113) Lian, Z.; Wei, C.; Gao, B.; Yang, X.; Chan, Y.; Wang, J.; Chen, G. Z.; Koh, K. S.; Shi, Y.; Yan, Y.; Ren, Y.; He, J.; Liu, F. Synergetic treatment of dye contaminated wastewater using microparticles functionalized with carbon nanotubes/titanium dioxide nanocomposites. *RSC Adv.* **2020**, *10* (16), 9210–9225.
- (114) Hossain, S.; Chun, D.-M. ZnO decorated polydimethylsiloxane sponges as photocatalysts for effective removal of methylene blue dye. *Mater. Chem. Phys.* **2020**, *255*, 123589.
- (115) Abdelhafeez, I. A.; Zhou, X.; Yao, Q.; Yu, Z.; Gong, Y.; Chen, J. Multifunctional Edge-Activated Carbon Nitride Nanosheet-Wrapped Polydimethylsiloxane Sponge Skeleton for Selective Oil Absorption and Photocatalysis. *ACS Omega* **2020**, *5* (8), 4181–4190.
- (116) Li, X.; Li, Y.; Huang, Y.; Zhang, T.; Liu, Y.; Yang, B.; He, C.; Zhou, X.; Zhang, J. Organic sponge photocatalysis. *Green Chem.* **2017**, *19* (13), 2925–2930.
- (117) Zhang, T.; Liang, W.; Huang, Y.; Li, X.; Liu, Y.; Yang, B.; He, C.; Zhou, X.; Zhang, J. Bifunctional organic sponge photocatalyst for efficient cross-dehydrogenative coupling of tertiary amines to ketones. *Chem. Commun.* **2017**, *53* (93), 12536–12539.
- (118) Yang, Y.; Zhang, Q.; Zhang, R.; Ran, T.; Wan, W.; Zhou, Y. Compressible and Recyclable Monolithic g-C₃N₄/Melamine Sponge: A Facile Ultrasonic-Coating Approach and Enhanced Visible-Light Photocatalytic Activity. *Front Chem.* **2018**, *6*, 156.
- (119) Cao, G.; Liu, Z. Floatable graphitic carbon nitride foam-supported BiOBr composites with high photocatalytic activity. *Mater. Lett.* **2017**, *202*, 32–35.
- (120) Li, F.; Lan, X.; Shi, J.; Wang, L. Loofah sponge as an environment-friendly biocarrier for intimately coupled photocatalysis and biodegradation (ICPB). *J. Water Process Eng.* **2021**, *40*, 101965.
- (121) Guo, S.; Li, X.; Li, J.; Wei, B. Boosting photocatalytic hydrogen production from water by photothermally induced biphasic systems. *Nat. Commun.* **2021**, *12* (1), 1343.
- (122) Zhang, G.; Choi, W. A low-cost sensitizer based on a phenolic resin for charge-transfer type photocatalysts working under visible light. *Chem. Commun.* **2012**, *48* (86), 10621–10623.
- (123) Olivo-Alanís, D.; Atilano-Camino, M. M.; García-González, A.; Humberto-Álvarez, L.; García-Reyes, R. B. Chlorophyll-sensitized phenolic resins for the photocatalytic degradation of methylene blue and synthetic blue wastewater. *J. Sol-Gel Sci. Technol.* **2021**, *100* (3), 538–554.
- (124) Tobin, J. M.; McCabe, T. J. D.; Prentice, A. W.; Holzer, S.; Lloyd, G. O.; Paterson, M. J.; Arrighi, V.; Cormack, P. A. G.; Vilela, F. Polymer-Supported Photosensitizers for Oxidative Organic Transformations in Flow and under Visible Light Irradiation. *ACS Catal.* **2017**, *7* (7), 4602–4612.
- (125) Wang, L.; Chen, X.; Duan, Y.; Luo, Q.; Wang, D. Macroporous polymer resin with conjugated side-chains: an efficient Ag nanoparticle support for preparing a photocatalyst. *Catal. Sci. Technol.* **2020**, *10* (13), 4191–4200.
- (126) Esen, C.; Antonietti, M.; Kumru, B. Upgrading poly(styrene-co-divinylbenzene) beads: Incorporation of organomodified metal-

free semiconductor graphitic carbon nitride through suspension photopolymerization to generate photoactive resins. *J. Appl. Polym. Sci.* **2021**, *138* (35), 50879.

(127) Esen, C.; Kumru, B., Thiol-ene Polymer Beads via Liquid-Liquid Printing: Armored Interfaces and Photopolymerization via Graphitic Carbon Nitride. *Nanoscale Adv.* **2022**, DOI: 10.1039/D2NA00254J.

Recommended by ACS

Postfabrication Functionalization of 4D-Printed Polycarbonate Photopolymer Scaffolds

Scott L. Brooks, Andrew C. Weems, *et al.*

JULY 27, 2022
ACS APPLIED POLYMER MATERIALS

READ 

Light-Directed Organization of Polymer Materials from Photoreactive Formulations

Ian D. Hosein.

MARCH 04, 2020
CHEMISTRY OF MATERIALS

READ 

Unclonable Features via Electrospraying of Bulk Polymers

Abidin Esidir, M. Serdar Onses, *et al.*

JUNE 30, 2022
ACS APPLIED POLYMER MATERIALS

READ 

Polymer Grafting to Polydopamine Free Radicals for Universal Surface Functionalization

Mitchell D. Nothing, Martina H. Stenzel, *et al.*

APRIL 11, 2022
JOURNAL OF THE AMERICAN CHEMICAL SOCIETY

READ 

Get More Suggestions >